

Article

Provenance Variability in Coeval Slope Channel Systems: Hermod S2 Member Sandstone (Eocene), South Viking Graben (North Sea)

Wiktor Marek Luzinski ^{1,*}, Andrew C. Morton ^{1,2,*}, Andrew Hurst ¹, Ingeborg Ims Tøllefsen ³
and John Cater ⁴

¹ Department of Geology and Geophysics, King's College, University of Aberdeen, Aberdeen AB24 3UE, UK

² CASP, West Building, Madingley Road, Cambridge CB3 0UD, UK

³ Aker BP ASA, Jattavagveien 10, Hinna Park, 4020 Stavanger, Norway

⁴ PetroStrat Ltd., Century House, Gadbrook Business Centre, Northwich CW9 7TL, UK

* Correspondence: w.luzinski.18@abdn.ac.uk (W.M.L.); heavyminerals@hotmail.co.uk (A.C.M.)

Abstract: Conventional and varietal heavy mineral studies of the earliest Eocene Hermod S2 Member (Mbr) sandstones in the Greater Alvheim area of the northern North Sea have revealed marked lateral variations and more subtle vertical evolution in provenance signature. Major variations are of geographic rather than stratigraphic nature as biostratigraphy reveals that all investigated sandstones are coeval. The provenance variations show an organized pattern, with sandstones in the north showing a different signature than those in the south. The position of the sandstones relative to the East Shetland Platform (ESP) is inferred to be the main control on provenance, with sediment input from at least two different point sources. Sediment supplied from both catchments is predominantly recycled in nature, given the mineralogical maturity of the heavy mineral assemblages, consistent with the evidence for widespread Permo-Triassic and Devonian sediments on the ESP. However, some direct supply from metasedimentary (Moine and Dalradian) basement is implied by the sporadic occurrence of unstable minerals. The southern catchment incorporated a greater exposure of Permo-Triassic sandstones than the northern catchment. The Permo-Triassic part of the catchment can be reconstructed as comprising equivalents of the Foula and Otter Bank sandstones present to the west of Shetland, with the majority of the Foula section having been stripped off prior to Hermod S2 deposition, exposing Otter Bank equivalents for erosion and redeposition. However, remnant Foula-like sandstones remained exposed further south on the ESP until at least the earliest Eocene since Foula-type garnet signatures are found in the Forties Sandstone Mbr of the central North Sea. In addition to lateral differences, stratigraphic evolution of provenance can also be detected in the Hermod S2 Mbr, with variations in key provenance-sensitive parameters related to a sea-level rise that reduced the extent of alluvial storage and altered the geological framework of the hinterland.

Keywords: provenance; stratigraphy; heavy mineral analysis; Eocene; Viking Graben; Hermod



Citation: Luzinski, W.M.; Morton, A.C.; Hurst, A.; Tøllefsen, I.I.; Cater, J. Provenance Variability in Coeval Slope Channel Systems: Hermod S2 Member Sandstone (Eocene), South Viking Graben (North Sea).

Geosciences **2022**, *12*, 450. <https://doi.org/10.3390/geosciences12120450>

Academic Editors:

Jesús Martínez-Frías and
Salvatore Critelli

Received: 27 October 2022

Accepted: 1 December 2022

Published: 6 December 2022

Publisher's Note: MDPI stays neutral with regard to jurisdictional claims in published maps and institutional affiliations.



Copyright: © 2022 by the authors. Licensee MDPI, Basel, Switzerland. This article is an open access article distributed under the terms and conditions of the Creative Commons Attribution (CC BY) license (<https://creativecommons.org/licenses/by/4.0/>).

1. Introduction

In the northern North Sea (UK Quadrant 9 and Norwegian Quadrant 25; Figure 1), hydrocarbon accumulations are prolific and associated with deep-marine sandstone deposited in channel and fan complexes [1–4]. The same stratigraphic interval is characterized by widespread sandstone intrusions [5–9], and the early Eocene Hermod S2 Member (Mbr) is postulated as a potential parent unit for several injection complexes in the Norwegian North Sea [10–12].

North Sea sandstone provenance evolved throughout the Palaeogene in response to geological changes in the hinterland related to the activity of the Icelandic Plume [1,2,13]. Stratigraphic evolution of provenance was, however, established only at the scale of the entire Palaeogene [14,15]. By contrast, investigations of provenance variations within

sandstones [15–19]; constraining parent units to sandstone intrusions; and investigating injection processes [20,21].

Heavy mineral provenance studies play an important role in evaluating and constraining the composition of source terranes and the modification of the detritus by weathering and erosion [16,19,22–24]. Mechanical and chemical modification of sand grains occurs during their transport from a source terrane to their deposition in a sedimentary basin, and heavy minerals are diagnostic of the effects of these processes [19,22]. Burial diagenetic processes further modify heavy mineral assemblages and their component grains [22,25–27].

Garnet geochemistry was chosen for varietal heavy mineral analysis. Garnet geochemical analysis has proven successful in discriminating and establishing provenance of North Sea Palaeocene sandstones [14,28–30]. Garnet varietal studies are based on chemical variations within this single mineral group, and they yield provenance-sensitive data for two reasons. First, the limited density range makes provenance signals invulnerable to sorting during transport [22,31], and second, garnet has relatively high chemical stability, making it applicable to sediments that suffered significant burial or prolonged storage in the alluvial basin. While studies have shown that calcium-rich end members dissolve preferentially [26,32] under deep burial conditions or during intense weathering, neither of these are the case in this study.

Other provenance techniques remain untested in the Palaeocene section of the North Sea, and no reference frameworks exist that would enable meaningful and reliable interpretation of obtained results.

2. Geological Setting

2.1. Basin Formation and Stratigraphy

A sedimentary basin in the North Sea Viking Graben developed during a major rifting event in the Late Jurassic [33], which likely accentuated pre-existing topography related to previous rifting events [34]. Rifting continued in pulses of faulting separated by periods of tectonic quiescence until the Early Cretaceous, but it failed to develop to the point of breakup. The Early Cretaceous marked the onset of rapid thermal subsidence, which lasted into the Palaeogene [34] and resulted in widespread transgression over the Viking Graben by the latest Jurassic [35]. Continued subsidence formed deep and broad marine basins, including the Viking Graben, bound to the west by a major fault complex, which appears to have controlled the shelf-edge position and basin profile [35,36].

North Sea Palaeogene depositional systems record a complex interplay of sediment supply, sediment composition, hinterland uplift and relative sea-level changes [1] as well as climate and differential basin subsidence and tilting [2,37]. The distribution of facies and sandstone bodies was largely controlled by pre-existing Mesozoic structures, evolving physiography, syn-depositional tectonics and local salt movements [2,35,37,38].

Sediment supply was largely controlled by uplift of the western and eastern basin margins [33]. While uplift of the East Shetland Platform, Scottish Highlands and Northern England was significant, uplift in Norway was more limited [1,2], and hence, the Scotland-Shetland hinterland acted as the primary source of sediment throughout Palaeocene and Lower Eocene [14]. The locus of hinterland erosion shifted during this period, with different source areas active at different times. The stratigraphically and laterally variable provenance of Palaeogene sandstones is reflected in the composition of heavy mineral assemblages and garnet suites [14,15,18]. Complexity in interpretation of Palaeogene heavy mineral assemblages in the North Sea is caused by post-depositional progressive dissolution of unstable heavy minerals with increasing burial depth and associated pore water temperature [25].

This study focuses on sandstone in the Hermod S2 Mbr, which exists over a large portion of UK Quadrant 9 and Norwegian Quadrant 25 (Figure 1). The Hermod Mbr (Figure 2) lies within mudstones of the Sele Formation and below the tuffaceous Balder Formation and intra-Balder sandstones of the Odin Mbr [3]. It has been dated as late Thanetian—earliest Ypresian and comprises a series of clean, structureless sandstones,

interbedded with thinly laminated claystones [3,39]. Hermod Mbr sandstones are deposits of submarine fan systems, with the more distal parts described as lobe deposits [3]. They are generally interpreted as systems of discrete feeder channels that transform into radiate fans, but they can form more amalgamated channel and lobe complexes [3,35].

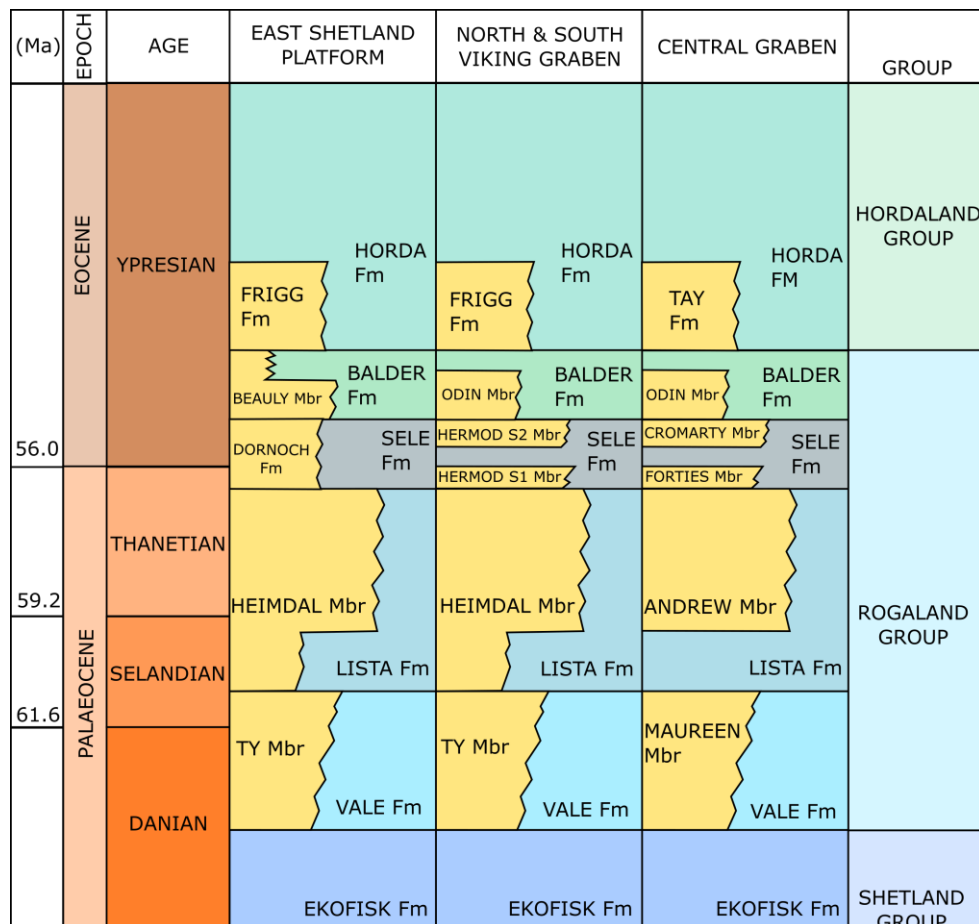


Figure 2. Stratigraphy of the Palaeogene interval of the investigated area showing the sandstone formations and members discussed in the text (sandstones shown in yellow). Other regions shown for correlation. Modified after Brunstad et al. [3], Deegan and Scull [40] and Hartog et al. [1].

Hermod Mbr sandstone occurs at two different stratigraphic levels within the Sele Formation (Figure 2) [3]. The two intra-Sele sandstone developments are differentiated on the basis of dinoflagellate biostratigraphy [3,39]. Hermod S1, which is the older depositional episode, lies below the first downhole appearance of abundant *Apectodinium augustum* [3,39]. It is stratigraphically equivalent to Skadan and Teal sandstones, which are found elsewhere in the northern North Sea and to the Forties Sandstone Mbr of the UK central North Sea [2]. Hermod S2 represents a later depositional episode and lies above the first downhole appearance of abundant *Apectodinium augustum*; Hermod S2 is an age equivalent of the upper Dornoch Formation and Cromarty Mbr sandstones in the UK sector of the North Sea [3,39]. Hermod S2 sandstones form laterally limited individual developments, often supplied by individual feeder channels (Figure 3), and are very strongly channelized with channels supported by well-developed levees. Clean sandstones are found in these channels as well as in braided frontal splays and sandstone intrusions [3,35].

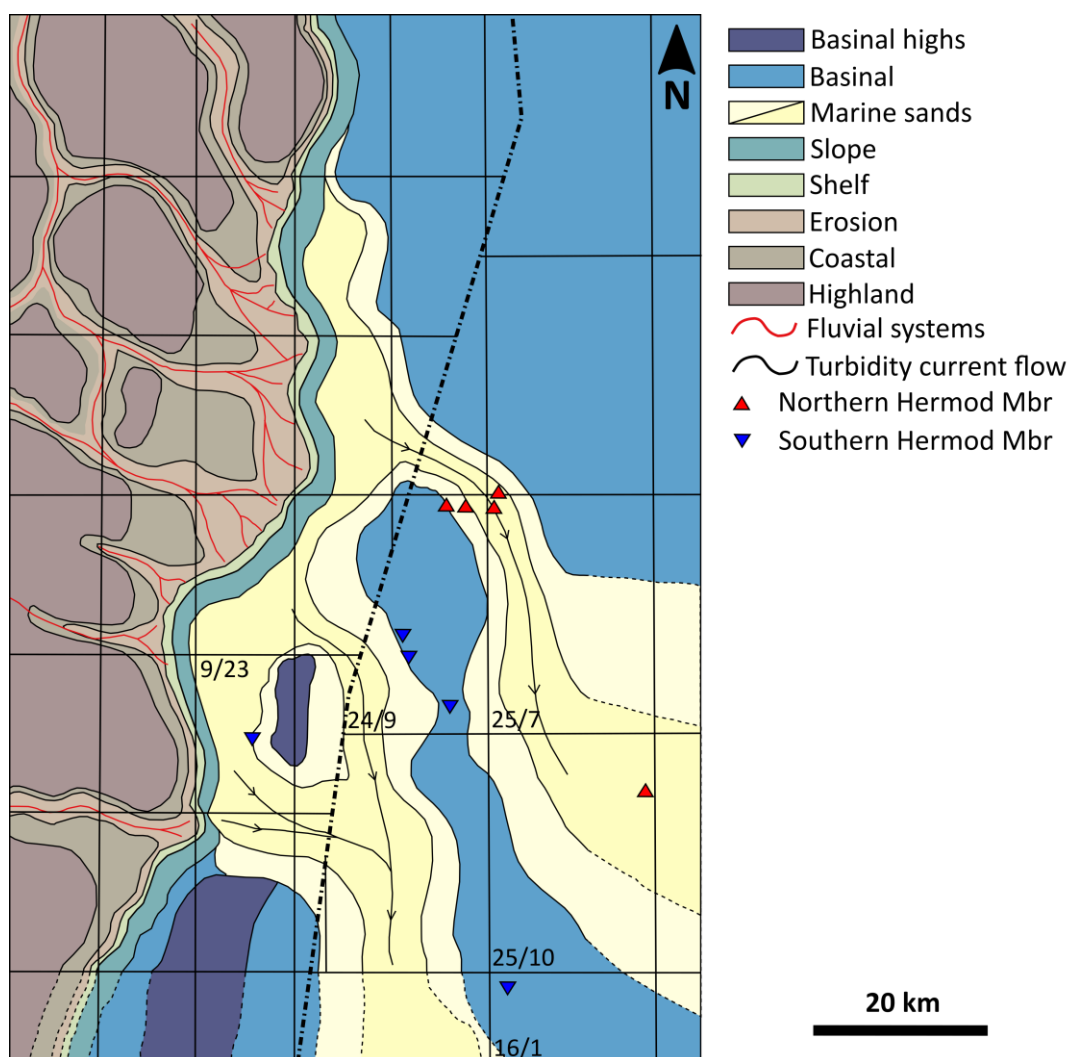


Figure 3. Depositional environment map of T48 sequence, corresponding to early Eocene (Ypresian). Key wells penetrating Hermod S2 Mbr are highlighted. Red triangles denote northern well group; blue inverted triangles denote southern well group (see text for definitions). Modified after Dixon & Pearce [41].

The sandstones that are the subject of this paper are ascribed to Hermod S2 Mbr. Biostratigraphic data from the Hermod Mbr of the Caterpillar and Bøyla discoveries (wells 24/9-10S and 24/9-9S, respectively; Figure 1) show that they all lie above the first downhole appearance of *Apectodinium augustum* [42,43]. Hermod Mbr sandstones in the Volund area (well 24/9-5; Figure 1) are also ascribed to Hermod S2 by correlation with offset wells (25/7-5 and 25/7-6) penetrating the Hermod Mbr in the vicinity of Kobra injectites [44].

2.2. Geology of the Hinterland

At present, the Shetland Isles outcrops consist of the metamorphic basement of Lewisian, Grenville, Moine and Dalradian strata; several major plutonic intrusions of variable age; sedimentary cover of Old Red sandstone (ORS); and an ophiolitic complex outcropping on Unst and Fetlar Islands [45]. Small outcrops of Lewisian and Grenville gneisses are found in the west and northwest of the Shetland Isles (Figure 4). Moine strata outcrop in the central and northern part of the Shetlands (Figure 4) and consist of schists and gneisses. Dalradian outcrops can be found in the southern and central part of the Shetlands (Figure 4) and include schists, gneisses, volcanics, quartzites and metasandstones [45]. The metamorphic grade of the basement is variable and reaches up to amphibolite facies [28].

Plutonic intrusions are found primarily to the west and north and include acidic and intermediate igneous rocks (Figure 4) [45]. Old Red Sandstone outcrops primarily to the west, east and south and is comprised of arenites and conglomerates dated to Middle Devonian (Figure 4) [45]. Ophiolites outcrop to the northeast on Unst and Fetlar (Figure 4) and include mantle rocks, metadunites, metagabbros, metasediments and some minor volcanic rocks; the metamorphic grade is generally low but can locally reach up to amphibolite facies [45–49].

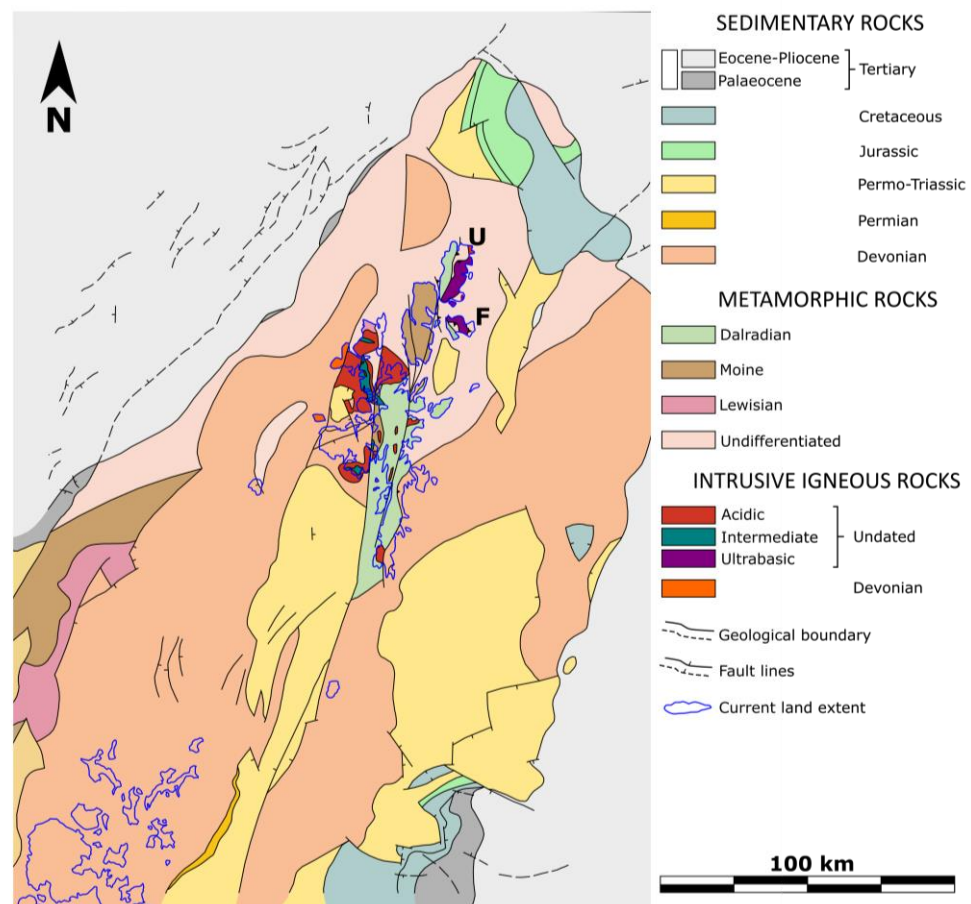


Figure 4. Simplified geological map of the hinterland (East Shetland Platform) and surrounding areas. Modified after Chesher [50]. U = Unst, F = Fetlar.

Geological maps of the offshore Shetland Platform indicate that metamorphic basement extends towards the north and west, where it gives way to Palaeogene and Neogene sedimentary cover (Figure 4). Sediments of Devonian age are the most extensive stratum and effectively flank the Shetland Isles to both east and west, constituting a major part of the ESP (Figure 4). While strictly Permian strata are rare, Permo-Triassic sediments are common and extensive, particularly to the south and southeast of the Shetland Isles (Figure 4). Jurassic and Cretaceous strata are rare and found only in the northeast and southeast of the ESP (Figure 4) [50].

3. Materials and Methods

32 core samples of Hermod S2 Mbr sandstones were analyzed in this study using conventional heavy mineral analysis (Figure 5). Of those 32 samples, 16 were chosen for varietal studies. Three extra samples from other sandstone Mbrs (Odin and Frigg) were analyzed through varietal HMA to provide context for a better interpretation of results. Clean sandstone samples most representative of the cored section were picked during sampling.

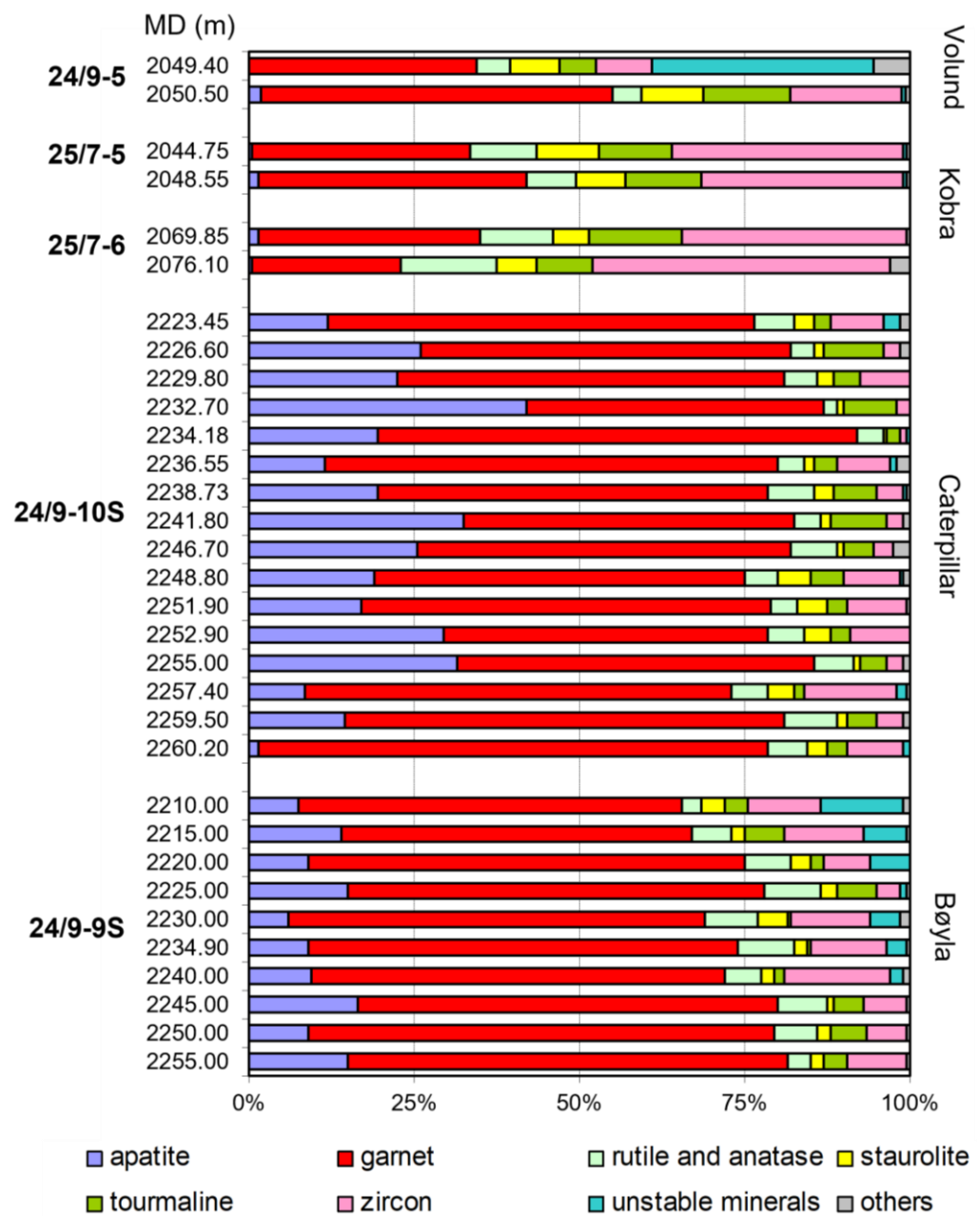


Figure 5. Heavy mineral assemblage compositions in the Hermod S2 Mbr in the Caterpillar discovery well, 24/9-10S, compared with equivalents elsewhere in the Greater Alvheim area. Note the markedly lower apatite and garnet contents and the correspondingly higher zircon, rutile and tourmaline abundances in the Volund and Kobra wells compared with Bøyla and Caterpillar, and also the high abundances of unstable minerals in one Volund sample. “Unstables” are amphibole, epidote and pyroxene. “Others” are allanite, corundum, chloritoid, gahnite, kyanite, monazite, sillimanite, titanite and xenotime.

Heavy mineral samples were prepared through density separation in bromoform following standard procedures described for example by Mange & Maurer [51], using the 63–125 micron grain size fraction. Conventional heavy mineral analysis was accomplished through identification and the counting of grains under a polarizing microscope using the Fleet method, where all grains in the field of view are identified and counted [52]. Mineral identification was made on the basis of optical properties, following Mange & Maurer [51]. For determination of percentage composition of the heavy mineral assemblage, no less than 200 grains were counted in each sample [31].

Heavy mineral assemblage compositions were augmented by determination of provenance-sensitive indices (Table 1), proposed by [31,51] to counteract the effects of processes that modify assemblage compositions during the sedimentary cycle and thereby obscure relationships between source rocks and sediment. Indices found to have value in the Hermod S2 Mbr are apatite:tourmaline (ATi), garnet:zircon (GZi) and rutile:zircon (RuZi). Following recommendations of Morton and Hallsworth [31], where possible 200 grains per mineral pair were counted, with 100 grains as minimal value for reliable index determination.

Table 1. Summary of heavy mineral indices discussed in this paper, after Morton and Hallsworth [31] and Morton et al. [53]. GZi, ATi and RuZi are provenance specific, whereas ZTi is affected by hydraulic conditions since it compares abundances of minerals with different densities. SZi is potentially controlled by diagenesis since staurolite is unstable during deep burial conditions [26].

Index	Mineral Pairs	Index Determination
ATi	Apatite, Tourmaline	% apatite in total apatite plus tourmaline
GZi	Garnet, Zircon	% garnet in total garnet plus zircon
RuZi	Rutile, Zircon	% rutile in total rutile plus zircon
SZi	Staurolite, Zircon	% staurolite in total staurolite plus zircon
ZTi	Zircon, Tourmaline	% zircon in total zircon plus tourmaline

Garnet analysis was conducted by electron microprobe analysis at Aberdeen University, following the method of Morton [29], with compositions expressed in terms of the four most common garnet end members: Fe-rich almandine, Mg-rich pyrope, Mn-rich spessartine and Ca-rich grossular. Garnet geochemistry gives insights on possible source lithologies, based either on known compositions of garnets from basement lithologies or from studies of modern river sediments and surficial sediments derived from potential hinterlands [28,32,54].

4. Regional Provenance Characteristics in Hermod S2 Mbr Sandstones

4.1. Conventional Heavy Mineral and Provenance-Sensitive Ratio Data

Two markedly different heavy mineral assemblage compositions are present in Hermod S2 Mbr sandstones in the more southerly Bøyla and Caterpillar fields compared with wells further north in Volund and Kobra fields. In Bøyla and Caterpillar, garnet is the dominant heavy mineral, with subordinate apatite, zircon, tourmaline and rutile (Figure 5). By contrast, heavy mineral assemblages in Volund and Kobra have significantly lower proportions of garnet and apatite, with correspondingly higher zircon, staurolite and tourmaline abundances. One of the Hermod S2 samples from 24/9-5 (Volund) is unlike any other in the data set, containing abundant diagenetically-unstable minerals, principally epidote but also calcic amphibole and clinopyroxene (Figure 5). A sample from Kobra (well 25/7-6) has higher zircon and correspondingly lower garnet proportions, but the assemblage from the other sample from this well is within the range present in the nearby Volund well (Figure 5).

The observed differences in Hermod S2 assemblages are further emphasized by provenance-sensitive indices GZi, ATi and RuZi. In Bøyla, these indices overlap with those in Caterpillar and form a distinctly different population to those in Volund and Kobra, which all have markedly lower ATi, GZi and RuZi indices (Figure 6). The Volund sample with abundant diagenetically unstable minerals falls close to the cluster defined by the other samples from this area, indicating that they have a common provenance (Figure 5). The presence of these unstable heavy minerals indicates that the sandstone unit was protected in some way from the high-temperature pore waters that dissolved them in the other samples, including the one only 1.10 m below.

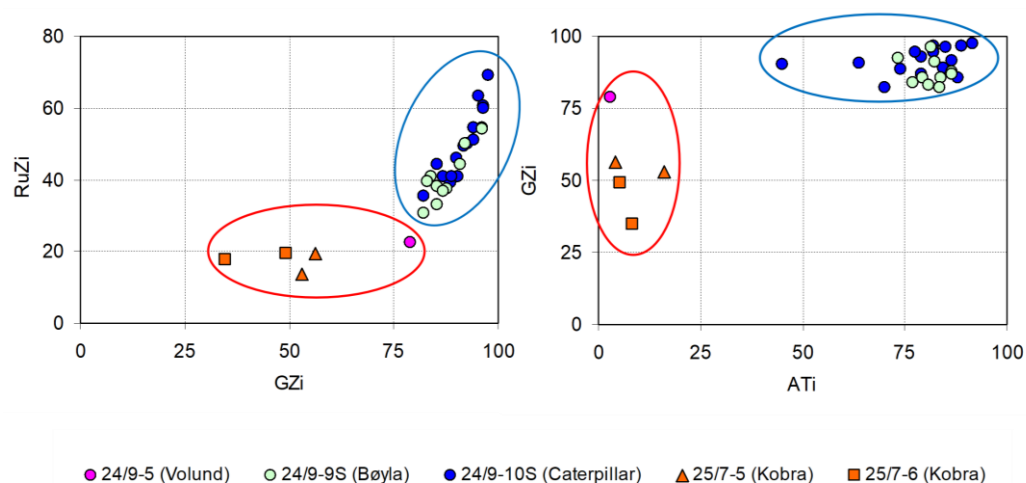


Figure 6. Crossplots of provenance-sensitive index parameters ATi, GZi and RuZi for Hermod S2 sandstones in the Greater Alvheim area. Note the marked difference between the characteristics shown by Caterpillar and Bøyla compared with Volund and Kobra. Based on clear differences in key HM indices, assemblages can be divided into northern Hermod S2 Mbr (circled in red) and southern Hermod S2 Mbr (circled in blue).

Based on heavy mineral assemblage compositions and heavy mineral indices, Hermod S2 Mbr sandstone can therefore be split into two groups with distinct provenance signature (Figure 6); these two groups have geospatial significance with clear variations between northern and southern wells (Figures 3, 5 and 6). The northern group comprises wells in Volund and Kobra; the heavy mineral assemblage is characterized by very high chemical maturity and depletion of apatite but invariably preserves staurolite and can preserve a high number of unstable grains. The southern group comprises wells in Bøyla and Caterpillar; heavy mineral assemblages are rich in garnet and apatite and display lower chemical maturity and more diversity than those of northern Hermod S2 Mbr (Figures 3, 5 and 6).

4.2. Garnet Assemblages

Garnet assemblages (Figures 7–9) also display marked differences between the northern and southern Hermod S2 Mbr. Although all the Hermod S2 assemblages are dominated by Type B garnets (Figures 7–9), those from the northern group contain fewer Type A and, to a lesser degree, Type C garnet (Figures 7–9). There is also a difference in relative proportions of Ca-poor and Ca-rich Type B garnets (Bi and Bii categories, respectively) between the southern and northern groups (Figures 7–9). In Caterpillar, samples from the upper part of Hermod S2 have more abundant Type C garnets compared with any part of the Bøyla succession, but the samples from the lower part of Hermod S2 are similar to Bøyla (Figures 8 and 9).

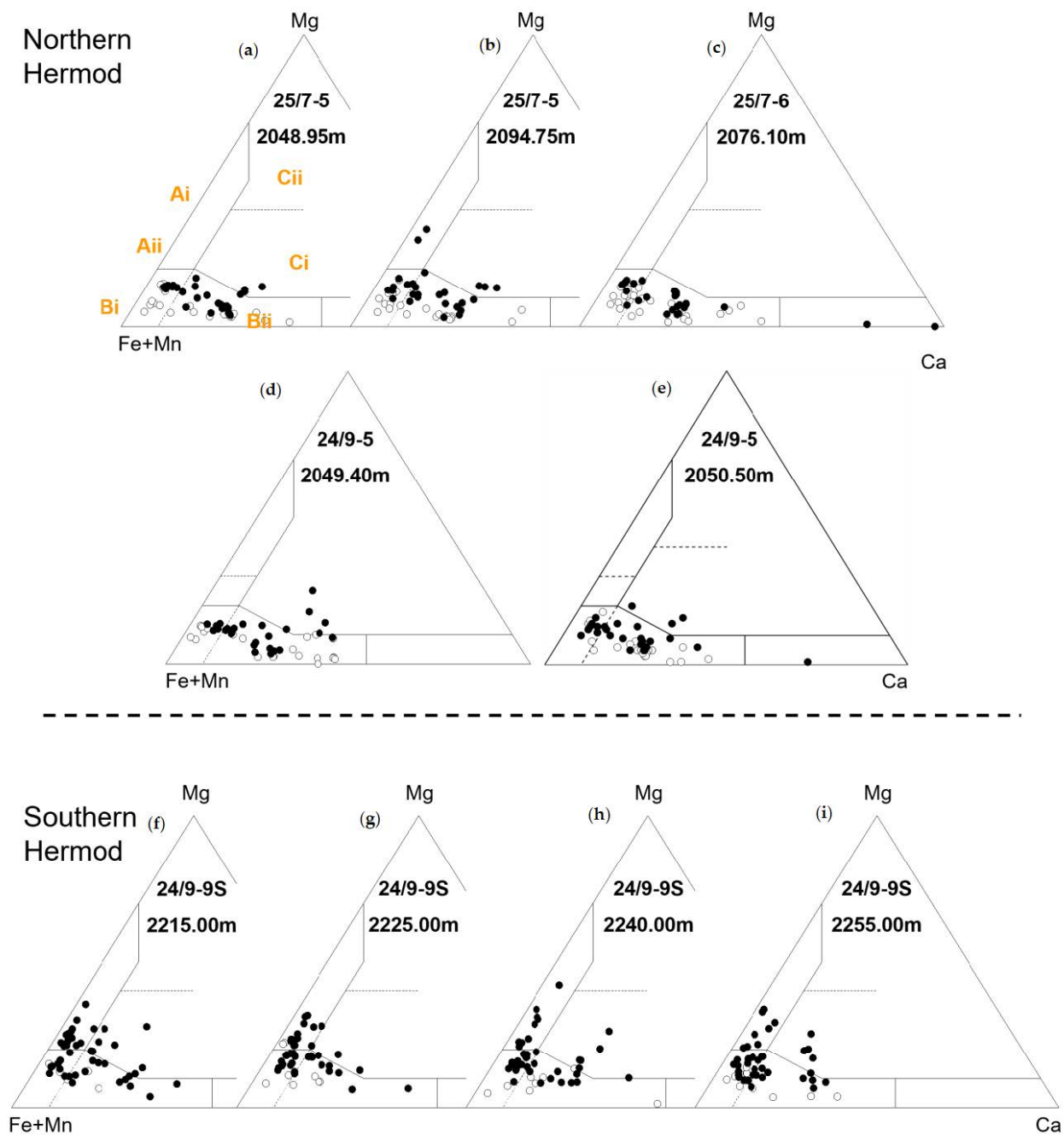


Figure 7. Ternary plots showing garnet assemblage compositions of Northern (a–e) and Southern (f–i) Hermod S2 Mbr. Northern Hermod S2 Mbr is found in Volund (24/9-5 and Kobra (25/7-5 and 25/7-6); samples from well 25/7-5 are examples of remobilized Northern Hermod S2 Mbr. Southern Hermod S2 Mbr is found in Bøyla (24/9-9S) and Caterpillar (24/9-10S). Mg—Pyrope, Fe + Mn—Almandine + Spessartine, Ca—Grossular. Filled circles—garnets with <5% Spessartine; open circles—garnets with >5% Spessartine. Garnet classification into types Ai, Aii, Bi, Bii, Ci and Cii is after Morton et al. [28], Jolley and Morton [55] and Mange and Morton [32].

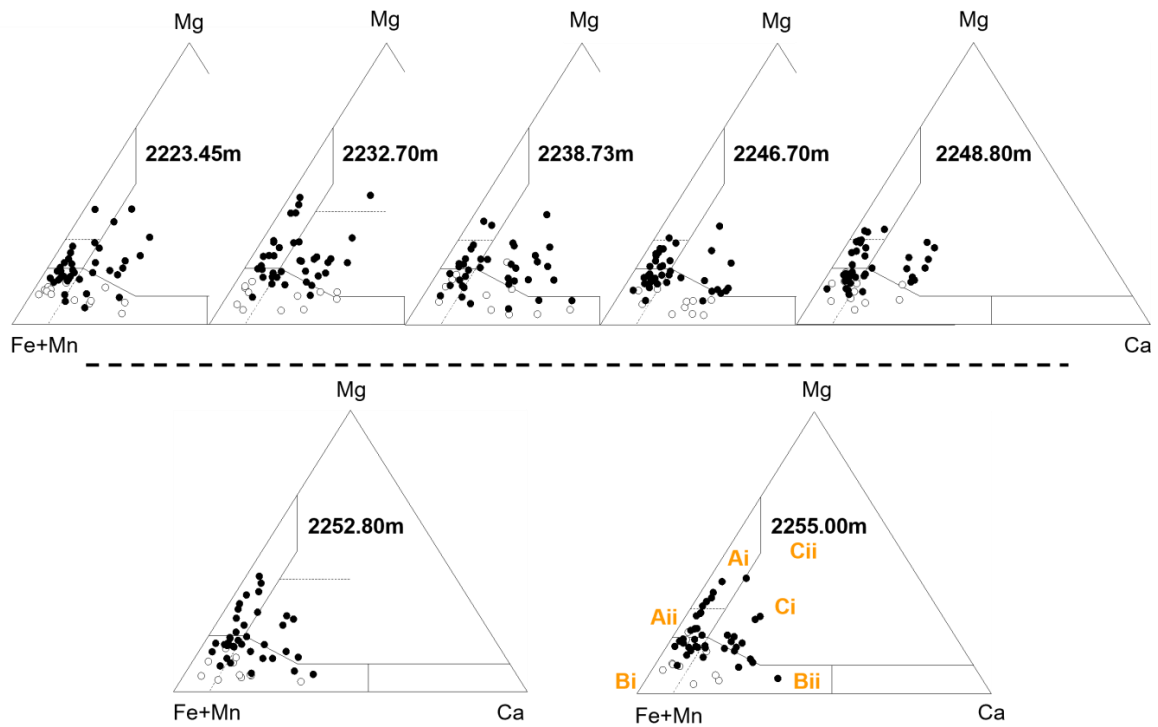


Figure 8. Ternary plots showing garnet assemblage compositions in the Hermod S2 Mbr of 24/9-10S, attributed to southern Hermod S2 Mbr. (Mg—Pyrope, Fe + Mn—Almandine + Spessartine, Ca—Grossular). Filled circles—garnets with <5% Spessartine; open circles—garnets with >5% Spessartine. Dashed line separates garnet assemblages showing signatures similar to Foula Fm (2252.80 & 2255.00 m) from those similar to Otter Bank Fm (2223.45–2248.80 m).

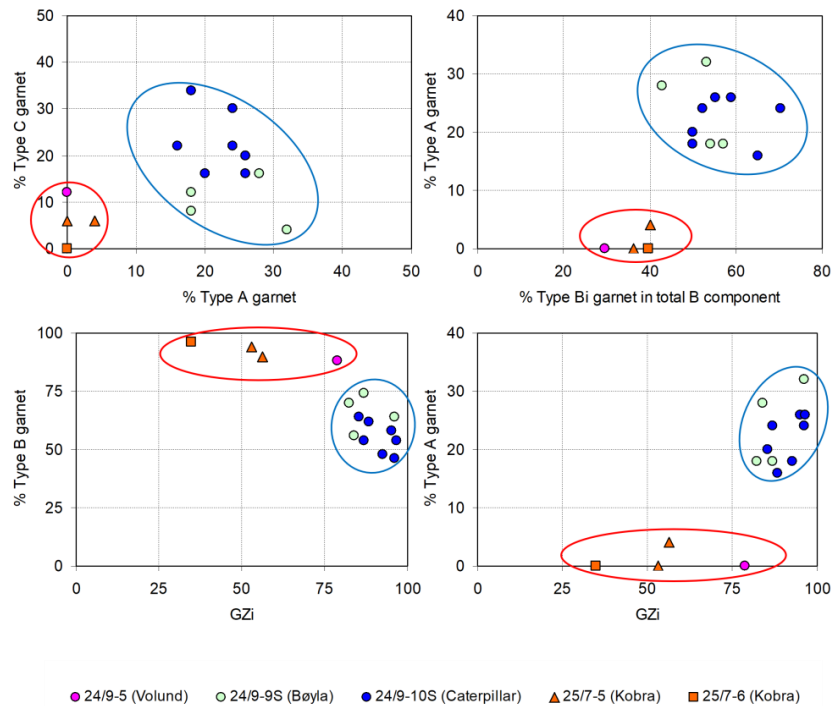


Figure 9. Plots of garnet assemblage compositions and GZi in Hermod S2 sandstones in the Greater Alvheim area. Note the marked difference between the characteristics shown by Caterpillar and Bøyla compared with Volund and Kobra. Based on clear differences in garnet compositions, assemblages can be divided into northern Hermod S2 Mbr (circled in red) and southern Hermod S2 Mbr (circled in blue).

4.3. Comparison with Regional Garnet Provenance Data

Morton et al. [14] (1993) found a clear evolution in garnet provenance during Palaeocene deposition in UK Quadrant 9 and adjacent Norwegian quadrant 25, the area encompassing the Bøyla, Caterpillar, Kobra and Volund discoveries (Figure 1). A series of mineral units (MT1-MT6) were defined on the basis of changes in garnet assemblages (Figure 9). Using biostratigraphic data, units MT1 and MT2 were ascribed to the lower and upper parts of the Maureen Formation (Ty Formation equivalent), respectively, with MT3, MT4 and MT5 belonging to the overlying Heimdal Formation [14]. Greater uncertainty concerned the stratigraphic affinity of Unit MT6, but it is now known that MT6 represents the Hermod S2 Mbr.

Garnet compositions in MT1 are heterogeneous, with Type A, B and C components all represented (Figure 10). MT2 has a distinctive garnet population dominated by Type Ai compositions, which give way to dominantly Type Aii in MT3. Units MT4 and MT5 show a progressive decline in abundance of Type A and an associated increase in Type B. This trend culminates with the virtually complete absence of Type A garnet in Unit MT6a (Figure 10), a feature that also characterizes younger sandstones in the area (Figure 10), notably the Odin Mbr (intra-Balder Formation) and the Frigg Formation (basal Hordaland Group). The regional garnet study demonstrates significant lateral heterogeneity in Hermod S2 Mbr mineralogy since assemblages dominated by Type Aii garnets were found in Norwegian well 16/1-1, defining mineral unit MT6b.

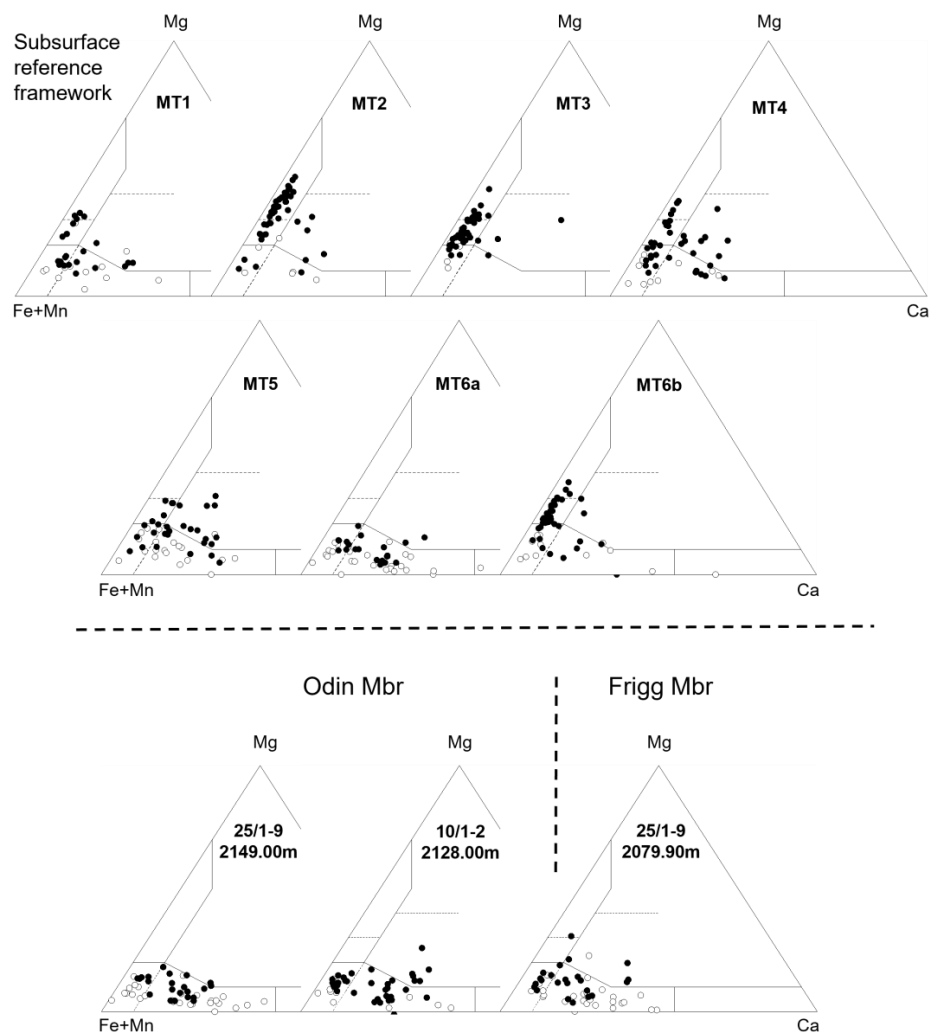


Figure 10. Evolution in Palaeocene-Early Eocene garnet provenance in UK Quadrant 9 and adjacent areas in the Norwegian sector of the North Sea, from Morton et al. (1993). Unit MT1 = Norwegian

well 26/4-1, 2253.0 m; Unit MT2 = UK Well 9/12-2, 2465.9 m; Unit MT3 = UK Well 9/13-1, 2252.5 m; Unit MT4 = UK Well 9/13-1, 2130.3 m; Unit MT5 = UK Well 9/23-1, 1905.0 m; Unit MT6a = Norwegian Well 25/10-1, 1786.8 m; Unit MT6b = Norwegian Well 16/1-1, 2347.0 m. Also shown are garnet assemblages from the Odin Member in Norwegian Well 25/1-9 (2149.00 m) and UK Well 10/1-2 (2128.00 m), plus the Frigg Member in Norwegian Well 25/1-9 (2079.90 m), respectively. Mg—Pyrope, Fe + Mn—Almandine + Spessartine, Ca—Grossular. See Figure 6 for the definition of garnet types.

A comparison of attributes of garnet assemblages in MT1–MT6 with those from Hermod S2 Mbr sandstones (Figure 11) demonstrates that garnets in MT2 and MT3 have significantly higher abundances of Type A grains than any Hermod S2 samples. Garnets in MT6b are similar, but not identical, to those in MT3. The southern Hermod S2 sandstones have similar garnet compositions to those seen in MT4 and MT5 as well as the basal Palaeocene MT1 unit, whereas garnets in the northern Hermod S2 sandstones are similar to those in MT6a.

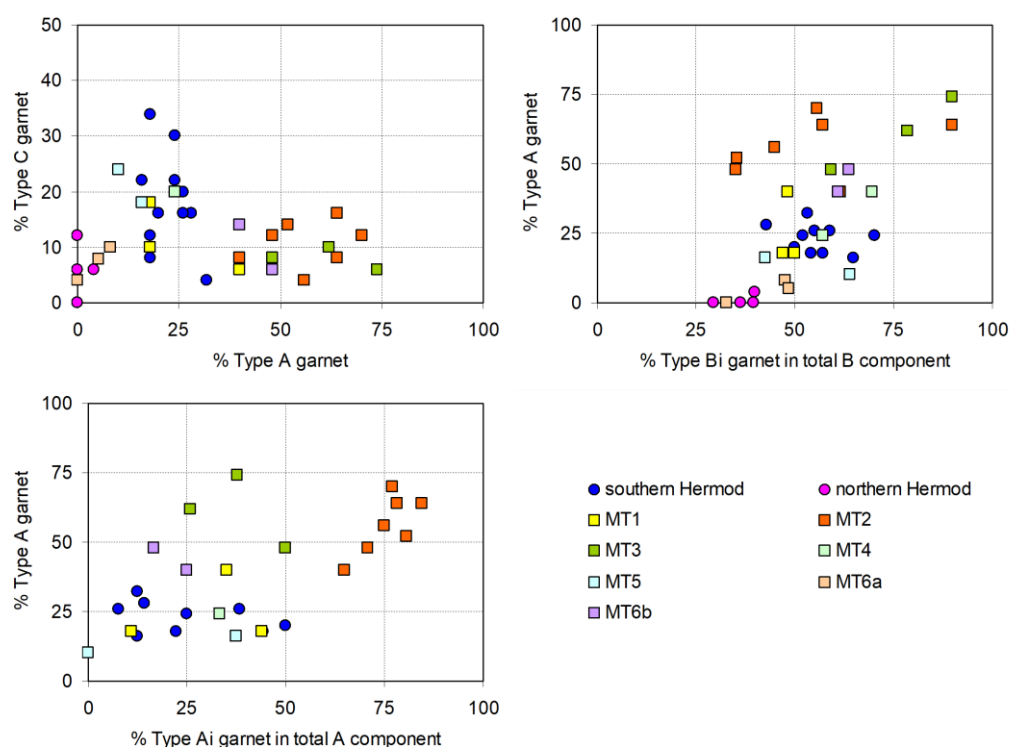


Figure 11. Comparison of garnet assemblage compositions in Hermod S2 sandstones with those found in Units MT1–MT6 (Morton et al., 1993). MT1 data from Norwegian wells 25/2-1 and 26/4-1; MT2 from UK wells 9/12-2 and 9/13-1; MT3 and MT4 from UK Well 9/13-1; MT5 from UK wells 9/13-1 and 9/23-1; MT6a from Norwegian wells 25/2-1 and 25/10-1; MT6b from Norwegian Well 16/1-1. Note the similarity between MT6a and the northern Hermod S2 group (Volund and Kobra) and between MT4/MT5 and the southern Hermod S2 group (Bøyla and Caterpillar).

5. Caterpillar Discovery Characterization

5.1. Sedimentology and Log Character

In the Caterpillar discovery well 24/9-10S, the Hermod S2 Mbr has been split into the “stratified upper Hermod S2 Mbr” and the “debrite-rich lower Hermod S2 Mbr” (Figure 12), based on changes in sediment type, sediment characteristics and sedimentary structures [56].

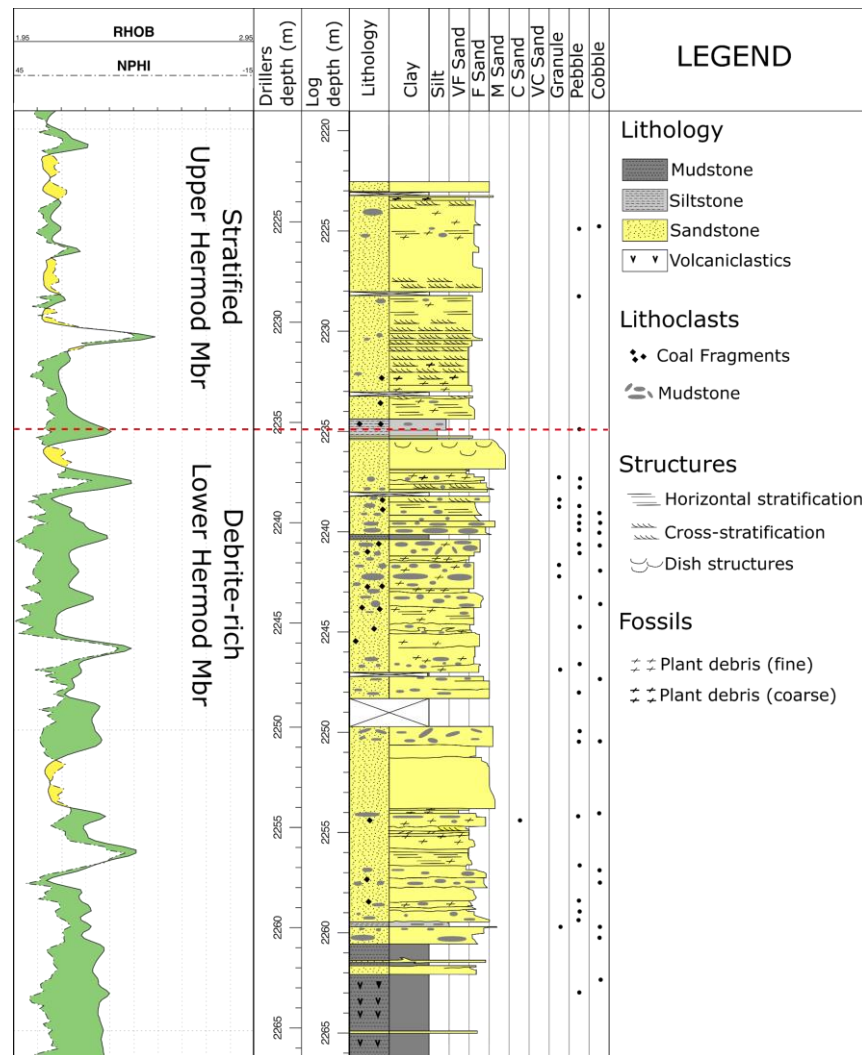


Figure 12. Overview log of the cored Hermod S2 Mbr, Caterpillar discovery, well 24/9-10S. The left-hand column shows a standard density-neutron geophysical log (RHOB—corrected bulk density, g/cm³; NPHI—Neutron Pula Hydrogen index, also known as compensated neutron porosity, *v/v*). Intervals with shale log response are coloured in green whereas those with sand log response are coloured in yellow. The boundary between the stratified Upper Hermod S2 Mbr and the debrite-rich lower Hermod S2 Mbr is marked by a red dashed line. Note a greater sand response in the upper part and the lower unit having more shale characteristics, most likely due to a very high proportion of shale debris.

The stratified upper Hermod S2 Mbr is composed of well-sorted, very fine to fine-grained sandstones. The sandstones are generally well-stratified, showing dense planar stratification or ripple lamination; structureless beds occur sporadically. Some pebbly beds are present, with clasts composed of Sele and Lista Fm mudstone fragments, as well as coaly debris. The sandstones are interpreted as deposits of proximally sourced low-density turbidites (Figure 12).

The debrite-rich lower Hermod S2 Mbr is an amalgamated succession of sandy turbidites and sandy debrites (Figure 12). The sandstones are moderately to well-sorted and fine- to medium-grained. Sandstone beds are generally structureless but frequently show weak normal grading. In some cases, structureless sandstones grade upwards into planar-stratified or ripple-laminated sandstones. Debritic beds are ubiquitous and are frequently associated with underlying sandy turbidites. Clasts, ranging in size from granules to cobbles and composed of Sele and Lista Fm mudstones and coaly debris, are present

in high concentrations. While the propensity of debritic beds decreases downhole, they remain a common feature (Figure 12). The debrite-rich lower Hermod S2 Mbr is interpreted as amalgamated deposits of high-density turbidites capped by linked debrites.

The debrite-rich lower Hermod S2 Mbr is interpreted as representing the progradation of terminal debrite-rich splay whereas the stratified upper Hermod S2 Mbr is interpreted as a feeder channel that supplied further prograding terminal splay deposits. The stratified upper Hermod S2 Mbr has slightly higher porosities and permeabilities than the debrite-rich lower Hermod S2 Mbr [56], but differences are minor, caused mainly by the presence of several impermeable samples within the lower unit.

5.2. Conventional Heavy Mineral and Provenance-Sensitive Ratio Data

Hermod S2 Mbr sandstones in Caterpillar have a rather narrow range in heavy mineral composition, characterized by high garnet concentrations, followed by apatite, zircon, tourmaline and rutile (Figure 5). There are variations between samples, but these do not define any obvious stratigraphic trends. However, application of the provenance-sensitive index method enables patterns to be more clearly observed. While average values across the sampled succession do not vary in a major way, there are sudden sample-to-sample changes in several indices that define clear breaks in trends (Figure 13). Most notably, at ~2235 m, ATi, RuZi and to a lesser degree GZi all show a sudden upward increase in values. This heavy mineral change corresponds to the boundary between the stratified upper Hermod S2 Mbr and the debrite-rich lower Hermod S2 Mbr, which is placed at 2235.41 m (Figures 12 and 13). There is another, more subtle change in GZi and RuZi between 2246.70 and 2248.80 m (Figure 12), but in this case, there is no associated change in ATi. However, ATi is distinctly lower in the basal part of the debrite-rich lower Hermod S2, especially in the deepest sample. These variations do not appear to directly correspond with any sedimentological boundary identified during the core study (Figure 12). SZi (staurolite:zircon index) displays a relatively consistent trend although values are slightly higher in the middle part of the Hermod S2 compared with the upper and lower parts (Figure 13), approximately corresponding to the interval with the highest amount of mudstone lithoclasts (Figure 12).

ZTi (zircon:tourmaline index), the other parameter displayed on Figure 13, is not an accurate provenance indicator because it is based on two minerals with contrasting densities and thus is strongly susceptible to hydrodynamic fractionation [21] as well as changes in source. The parameter shows sudden large-magnitude changes that are considerably more exaggerated than variations shown by the other indices, reflecting the major hydrodynamic control on this parameter. Nevertheless, ZTi clearly picks out the boundary between the stratified upper Hermod S2 and debrite-rich lower Hermod S2 Mbrs.

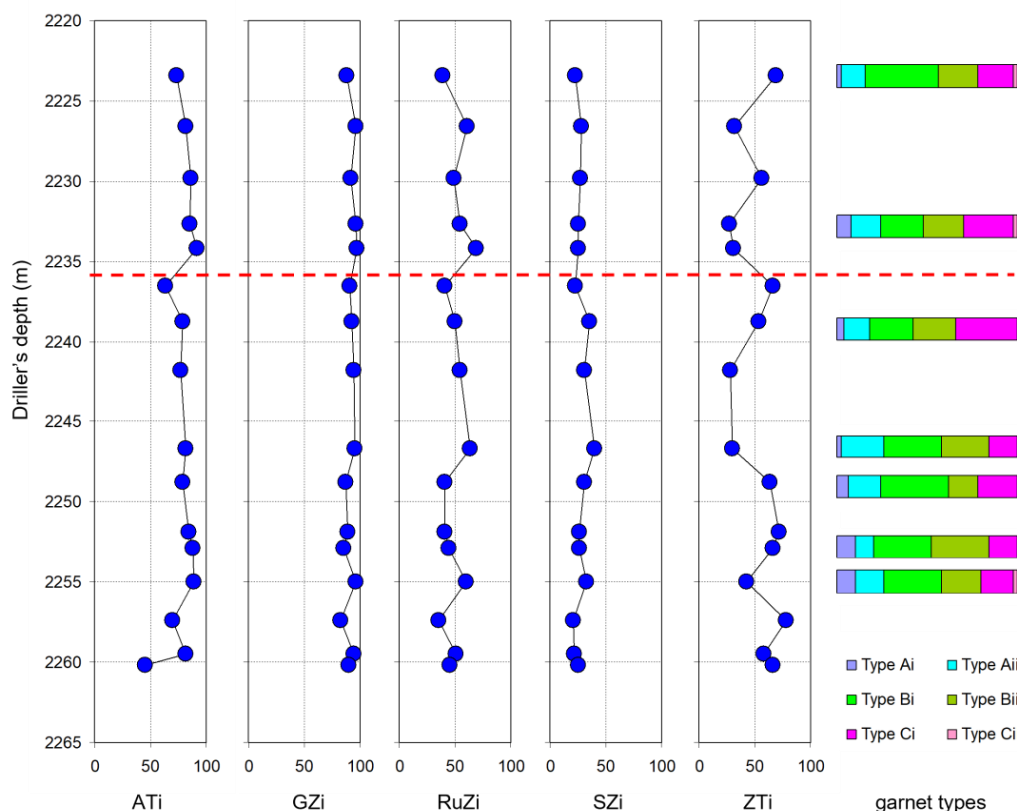


Figure 13. Stratigraphic variations in heavy mineral indices and garnet assemblage compositions in the cored Hermod S2 Mbr in Caterpillar discovery well 24/9-10S. The red dashed line marks the boundary between the upper stratified section and the lower debrite-rich interval. See Figure 6 for the definition of garnet types Ai, Aii, Bi, Bii, Ci and Cii.

5.3. Garnet Compositional Data

Garnet assemblages of Caterpillar Hermod S2 Mbr (Figure 8) are dominated by Type B compositions, with Bi and Bii in approximately similar proportions (Figures 8 and 9). Type A garnets are present in subordinate amounts, with Aii generally more common than Ai. Type C garnet is also conspicuous, especially in the shallower part of Hermod S2. The increase in abundance corresponds with an upward decrease in abundance of mudstone lithoclasts (Figure 12) but takes place below the heavy mineral event that correlates with the boundary between the stratified upper Hermod S2 and the debrite-rich lower Hermod S2 (Figure 13).

6. Discussion

6.1. Controls on Provenance Variations in the Hermod S2

Provenance variations similar to those present in Hermod S2 were observed in intra-Sele Formation sandstones in the central North Sea [30], in which garnet assemblages are almost identical to those described here. Some samples have extremely restricted Type B garnet assemblages, while others preserve diverse garnet compositions. Kilhams et al. [30] postulated that lateral versus axial sediment routing was the major control on garnet assemblages and their provenance. Diverse garnet assemblages in the axially sourced sandstones were attributed to derivation from Moine and Dalradian basement terrane combined with recycling of Triassic strata located on the East Shetland Platform (ESP). Restricted assemblages with exclusively Type B garnet were attributed to laterally sourced sand derived from the Dalradian terrane in the Grampian Highlands [30].

The model of lateral and axial interplay of source terranes in the intra-Sele of the central North Sea [30] is unlikely to be applicable to Hermod S2 sandstones in the South

Viking Graben. Axial supply has been postulated for the Heimdal Formation [57], but the N-S axis of the South Viking Graben is not obviously spatially associated with potential source terranes. All sandstones investigated herein are located such that sediment was most likely supplied laterally from the ESP. Detritus derived from the main Scottish landmass would have to be introduced to the basin from the southwest at an angle highly oblique to the basin axis. This is incompatible with the current understanding of basin tilt and general transport direction for Palaeocene and Eocene sandstones of the Viking Graben, which indicates the basin was tilted toward the southeast and sediment transport direction generally followed that slope [1,58]. Nevertheless, Kilhams et al. [30] is a useful starting point for developing models that could be applied to Eocene sandstones of the South Viking Graben. We believe that linking the provenance of sediment to specific regions on the ESP could account for lateral provenance signature variations of Hermod S2 sandstones investigated herein. Two models are conceived to explain the variations revealed in this study.

Model 1 This invokes contemporaneous or near-contemporaneous deposition of all Hermod S2 sandstones from distinct point-sources on the ESP, each with unique heavy mineral signatures and garnet assemblages (Figure 14a). In this scenario, the northern Hermod S2 sandstones formed a discrete system, point-sourced from a catchment on the central/northern ESP, whereas the southern Hermod S2 sandstones formed a separate system, sourced from a catchment on the central/southern ESP. This is consistent with existing interpretations of the geometry of the Hermod S2 Mbr, which supports deposition of sandstones in a strongly segmented system of confined lobes and channels that were derived from individual point sources on the ESP [1,3,35,41].

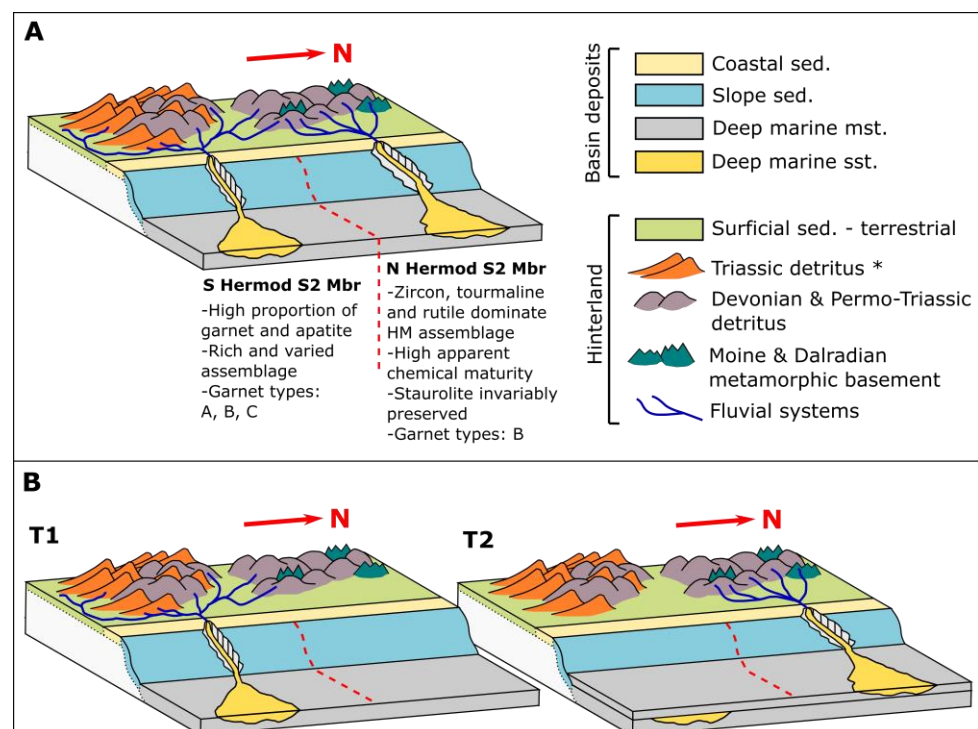


Figure 14. Alternative models for deposition of Hermod S2 Mbr sandstones. (A) Contemporaneous or near-contemporaneous deposition from distinct point sources. (B) Stratigraphic evolution of provenance and a northward shift of depocenter. * Triassic detritus specifically equivalent to Otter Bank & Foula Fms, bearing garnet assemblages rich in types A and C garnets.

Model 2 The evolution of provenance during the deposition of Hermod S2 sandstone is invoked (Figure 14b) with a major shift of source terrane occurring between sedimentation in the two areas. Biostratigraphic data show that sandstone in the Hermod S2 Mbr occurs in different stratigraphic positions [3], so it is conceivable that provenance switched between

different parts of the ESP. The change in provenance signature would be accomplished either by northward migration of the point-source or by differing activity of the point-sources through time. In this model, southern Hermod S2 sandstone is inferred to be older than northern Hermod S2 sandstone. Variations in provenance-sensitive indices and garnet compositions in the Caterpillar discovery well strongly indicate that provenance evolved through time (Figures 8 and 13).

Available biostratigraphic data suggest that all Hermod Mbr sandstones investigated herein are the younger S2 division, deposited during the earliest Eocene [42,43]. They have a very similar position with respect to specific palynological events, which implies they were deposited contemporaneously or near-contemporaneously. If any lag time separated deposition of the northern and southern examples, it was short; hence, the hypothesis of stratigraphic control on the provenance signal is hard to sustain. We infer that the extent and geology of the catchment areas supplying the northern and southern Hermod S2 sandstones must have been different and acted as a primary control on their contrasting provenance signature. Nevertheless, there is likely to have been some overlap, either partially shared drainage areas or outcrops of similar strata present in both catchments, since southern and northern Hermod S2 Mbr sandstones share some provenance characteristics, most notably the abundant Type B garnets (Figures 7–9). There is, however, evidence of a subtle difference in proportions of Ca-poor and Ca-rich Type B garnets between the two areas (Figure 9).

6.2. Stratigraphic Evolution of Hermod S2 Mbr Provenance Signature in Caterpillar

Deposition of the earliest Eocene fans, such as those containing the Hermod S2 Mbr, took place during a small-scale transgression associated with tectonic uplift [1]. The small-scale transgression occurred during the global Palaeocene-Eocene Thermal Maximum (PETM) that caused perturbation of the carbon cycle, climate and biosphere [59]. Drainage basins increased run-off rates and contributed to a global mobilization of clastic and dissolved sediment loads [60]. Kaolinite, an indicator of increased temperature and humidity in weathering environments, commonly increased in abundance in fine-grained sediment [61–63]. Deep weathering of a Danian sand injection complex caused the dissolution of originally diverse heavy mineral assemblages and was inferred to be associated with the PETM [21]. Ultrastable assemblages (zircon, tourmaline, rutile, garnet) prevailed whereas less chemically stable heavy minerals (apatite, epidote, titanite) became scarce or deeply etched.

In Caterpillar (well 24/9-10S), changes in ATi, GZi and RuZi at 2235 m coincide with the boundary between the “stratified upper Hermod S2 Mbr” and the “debrite-rich lower Hermod S2 Mbr” (Figure 12). Changes in GZi and RuZi are usually considered to reflect changes in provenance as the indices are generally deemed as unsusceptible to modification by hydrodynamic fractionation, weathering or diagenesis [22,31]. ATi is considered unsusceptible to hydrodynamic fractionation because apatite is extremely susceptible to acidic leaching and dissolves quickly during subaerial exposure [16]. Hence, ATi may respond to changing conditions during transport, with lower ATi indicating more exposure to acidic leaching during alluvial storage [16].

The sudden upward increase in ATi seen in Caterpillar at the boundary between the “upper” and “lower” Hermod S2 Mbr could be explained by sea-level rise, change in weathering conditions at source and in the alluvial basin or both. All these could potentially be linked to climatic changes surrounding the PETM; decrease in global temperatures towards the end of the PETM could account for decreased weathering of apatite at source and in alluvial storage [61,64]. The PETM was also associated with global sea-level rise [61,65–67], which likely culminated towards the end of the PETM. Regardless of the driving mechanism, a rise in sea level would shorten the transport distance in the alluvial drainage basin, leading to reduced exposure to acidic leaching and better preservation of apatite during transport [16]. As a change in ATi is accompanied by changes in GZi and RuZi, generally considered either less susceptible (for GZi) or resistant (RuZi) to weathering during transport, a component

of what is likely a small provenance change is also preserved. This change in provenance could also be related to the rise in relative sea level as it might be linked to geomorphological changes in the hinterland, either as the cause or effect thereof; as aforementioned, this change in sea-level could possibly be linked to the PETM [61,65–67]. Nevertheless, the provenance shift was small, as garnet assemblages investigated above and below the boundary are similar, and a common source terrane is inferred. Likewise, we postulate that the low ATi value in the lowermost Hermod S2 sample (Figure 13) is likely to reflect an influx of more weathered sediment stripped off from the alluvial basin in the initial phase of Hermod S2 sedimentation; this high intensity of weathering prior to deposition could again be linked to influence of hot-humid PETM climate [61,64].

The significance of other variations of indices is less clear. Minor hydrodynamic control may be inferred from the trends in RuZi, and to a lesser extent GZi, which mirror the ZTi trend (Figure 13). The trends of these indices may relate to the slightly different density of rutile and garnet compared with zircon [22]. The increase in abundance of Type C garnet within the mid-part of the Hermod S2 Mbr (Figure 13) is almost certainly attributable to a minor change in provenance.

6.3. Provenance of Hermod S2 Mbr Sandstone

Hermod S2 Mbr heavy mineral assemblages are rich in the ultra-stable minerals zircon, rutile and tourmaline, indicating high chemical maturity [22,31,68], especially in the northern group of wells (Figure 5). One explanation for the prevalence of ultra-mature heavy mineral assemblages is the effect of burial diagenesis [22,25,26]. Here, that is discounted because the sandstones were not buried to more than ~2400 m, as shown by the presence of staurolite, a moderately unstable mineral during burial diagenesis [22,25,26]. Apatite, which is stable during burial diagenesis [16,25,26], is a minor component, especially in the northern Hermod S2 area. This evidence supports that the high proportion of ultra-stable heavy minerals is provenance related, attributed either to recycling of pre-existing sediment present on the ESP or to extensive weathering of detritus during storage in the alluvial basin. Extensive weathering likely occurred for some of Palaeocene and Eocene sediments due to the hot-humid climate prevalent during the PETM [61,64]. Some first-cycle input from crystalline basement is identified since unstable minerals (epidote, amphibole and pyroxene) are present in the Hermod S2 sandstone sample from Volund that did not undergo extensive mineral dissolution (Figure 5). A combination of recycled and first-cycle detritus is consistent with the geological framework of the ESP (Figure 4), which consists largely of Permo-Triassic and Devonian sediments with Moine, Dalradian and minor Lewisian basement exposed on the Shetland Isles [50].

Further constraints on Hermod S2 sandstone provenance are given by their garnet assemblages. The prevalence of Type A garnets in North Sea sandstones, including the Jurassic [69] and the Palaeocene [14,27,30], is anomalous with respect to Scottish basement sources since modern rivers from Scotland and Shetland have scarce amounts of Type A garnet [28] (Figure 15). Triassic sandstone on the northwest margin of the UK continental shelf is commonly characterized by Type Ai-dominated garnet assemblages (Figure 15), such as the Foula Formation west of Shetland [70] and likely correlatives in the Rockall Basin and north of the ESP [71]. These are attributed to sources to the west and northwest of the British Isles. Garnet assemblages in the Foula Fm and equivalents are directly comparable to those found in Palaeocene sandstone in unit MT2 of Morton et al. [14]. The recycling of Triassic sandstone previously deposited on the ESP is therefore the only feasible explanation for the occurrence of sandstone with this type of garnet assemblage. The marked decline in abundance of Type Ai garnet in the later part of the Palaeocene suggests that Foula-type Triassic sandstone was largely stripped away from the catchment supplying the northern North Sea although it must have persisted further south on the ESP since Type Ai garnets remain common in the Hermod S2-equivalent Forties Sandstone Mbr in the central North Sea Palaeocene [27,28,30].

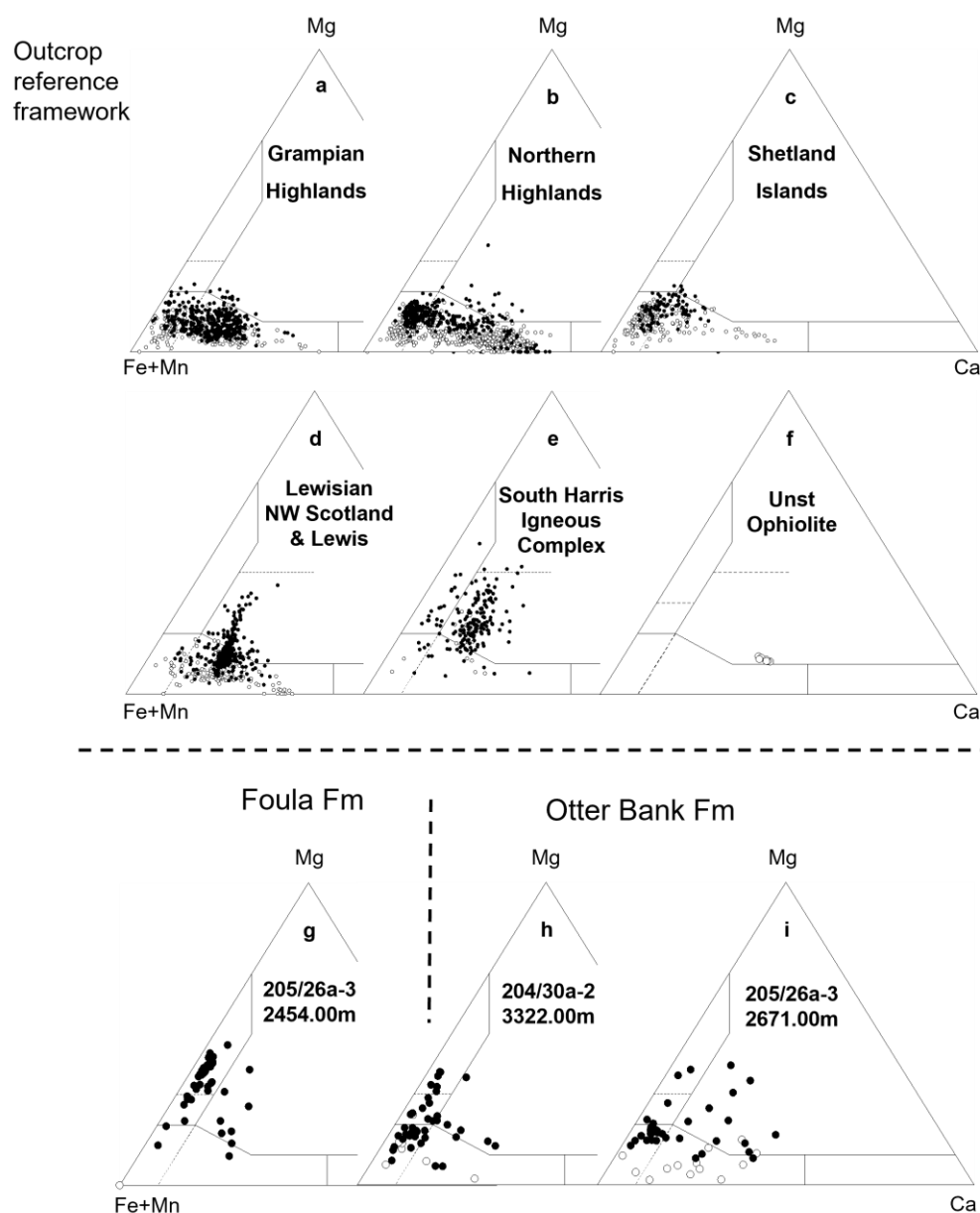


Figure 15. Garnet assemblages in modern river sediments draining Lewisian, Moine and Dalradian basement rocks of northern Scotland and the Shetland Isles, plus garnets in the Triassic Foula and Otter Bank Formations (west of Shetland) and the Unst Ophiolite (Shetland) from Morton et al. [28], Morton et al. [70] and Spray [49]. (a) Rivers draining the Grampian Highlands (predominantly Dalradian-sourced); (b) Rivers draining the Northern Highlands (predominantly Moine-sourced); (c) Rivers draining Dalradian and Moine rocks on Shetland; (d) Rivers draining Lewisian basement of northwest Scotland and Lewis; (e) Rivers draining the South Harris Igneous Complex; (f) garnetiferous facies of the Unst Ophiolite, Shetland; (g) Foula Formation in UK Well 205/26a-3 (2454.0 m); (h) Otter Bank Formation in 204/30a-2 (3322 m) and (i) Otter Bank Fm in 205/26a-3 (2671.6 m). Mg—pyrope, Fe + Mn—Almandine + Spessartine, Ca—Grossular. See Figure 6 for definition of garnet types. Filled circles—garnets with <5% Spessartine; open circles—garnets with >5% Spessartine.

The Early Triassic Otter Bank Formation conformably underlies the Foula Formation to the west of the ESP. Otter Bank sandstones lack common Type Ai garnets and have assemblages rich in Type B garnet with variable but subordinate amounts of Type Aii and Type C (Figure 15). Recycling of sandstone with Otter Bank characteristics is therefore a

likely origin for the younger Palaeocene and Eocene sandstone in the study area, including those in the Hermod S2 Mbr. Removal of the overlying Foula equivalent during the preceding Palaeocene would have exposed this older succession. A component of direct sourcing from Moine/Dalradian basement is inferred on the basis of the presence of unstable minerals unlikely to survive previous sedimentation cycles; such material has almost exclusively Type B garnet assemblages (Figure 15).

While less common than Type A garnet, Type C garnet constitutes a significant proportion of some Hermod S2 Mbr samples, notably those in the upper interval in Caterpillar. Type C garnet is typically associated with metabasic rock [32,54]. On the ESP, metabasic rocks are present as part of the Unst Ophiolite in northern Shetland, but generally the metamorphic grade is too low for extensive garnet formation [47–49]. While some garnetiferous outcrops of amphibolite facies hornblende-schists are found on Western Fetlar (Shetland), they are not widespread [46–48]. Microprobe analysis of garnets from the Fetlar outcrop shows no similarity with the majority of Type C garnets present, either in the Hermod S2 Mbr or in other Palaeocene-Eocene sandstone (Figure 15) [28]. The ultimate origin of Type C garnet in the North Sea Palaeocene-Eocene is likely to be the Lewisian gneiss of western Scotland and the Western Isles (Figure 15). While direct supply from the Lewisian cannot be entirely ruled out, recycling of garnet ultimately derived from the Lewisian is considered most likely.

7. Conclusions

Conventional and varietal heavy mineral analysis has revealed significant spatial variations in the provenance signature of sandstones attributed to the earliest Eocene Hermod S2 Mbr in the south Viking Graben. These variations form a consistent geographical pattern, with sandstones to the north showing different provenance signatures than those in the south. As biostratigraphic studies indicate that the investigated sandstones are of near-identical age, it is unlikely that there was a stratigraphic control on the variable provenance signature of sandstones in question. Instead, we propose that position of the sediment relative to the ESP and the location of the point sources on the shelf were the main controls on their provenance signature.

Sandstones in the north of the study area (Volund and Kobra) were supplied from point source(s) along the central to northern part of the ESP. The hinterland that provided sediment to these sandstones encompassed strata supplying almost exclusively Type B garnets. The ultimate provenance of such material is Moine and Dalradian basement, but the mineralogical maturity of the heavy mineral assemblages indicates that a significant proportion of the detritus was recycled from Devonian and Permo-Triassic strata on the ESP. Some direct supply from metamorphic basement is also likely given the sporadic presence of unstable minerals.

Sandstones further south (Caterpillar and Bøyla area) were supplied from point-source(s) along the southern-central ESP. The hinterland that provided sediment to these sandstones contained a wider range of strata compared with the northern source, as witnessed by a smaller ultrastable mineral component and a wider range of garnet compositions (Type B dominant but supplemented by Aii, C and, to a small degree, Ai). Recycled Triassic (Otter Bank equivalent) is likely to have been a major component, together with Devonian sediments and metamorphic basement.

As both sandstone groups contain a large Type B garnet component, it is likely that there was some overlap in characteristics of the source material. This could be either due to partially shared catchment area, sharing of some of the point sources or similar geology outcropping in both hinterlands. However, there are differences in the nature of the Type B garnets (Bi relative to Bii) between the two groups, suggesting the shared character is of limited extent.

Hermod S2 Mbr sandstones in the Caterpillar discovery well show a detectable vertical variation of provenance, even within a single channel. Abrupt changes in heavy mineral index values occur across the boundary between the lower debrite-rich interval and the

upper stratified interval. The increased ATi across this boundary suggests a decrease in the extent of hot-climate weathering, decreased alluvial storage related to sea-level rise or both. These could potentially be linked to climatic perturbation and sea level rise associated with the PETM. Change in ATi in Caterpillar are accompanied by slight increases in GZi and RuZi, reflecting small change in provenance likely driven by change in the drainage basin associated with potential sea level rise. Detailed investigation of this Hermod S2 sandstone section has revealed how the interplay of provenance change, sea-level change and related changes in drainage and transport system have controlled the composition of the heavy mineral assemblage and some heavy mineral parameters.

The Hermod S2 sandstones described in this study record part of the overall evolution in sediment provenance character during the Palaeocene and Early Eocene, as previously described by Morton et al. [14]. After initial heterogeneity in sourcing that supplied the basal Palaeocene sandstones (Unit MT1), there was a sudden major influx of sediment dominated by Type Ai garnet interpreted as recycled Foula-equivalent Triassic sandstones previously deposited on the ESP. In the study area, this ceased at the base of the Heimdal Fm to be replaced by sandstones with Aii garnet character, interpreted as indicating that all Foula sandstone had been stripped off from the catchment area. However, such material remained exposed further south on the ESP at least until the earliest Eocene since Ai garnets form an important component in the Hermod S2-equivalent Forties Sandstone Mbr in the central North Sea. The sandstones in units MT3, 4 and 5 record the progressive decline in Aii garnets and a concomitant increase in garnet Type B, locally with Type C, related to further unroofing on the ESP together with direct input from metamorphic basement. This record of unroofing provides strong evidence that strata, previously hypothesized to have outcropped on the ESP, were indeed of Triassic age as the observed provenance evolution pattern is consistent with the unroofing of two Triassic Fms that occur in stratigraphic sequence elsewhere.

Author Contributions: Conceptualization, W.M.L. and A.C.M.; methodology, W.M.L. and A.C.M.; software, N/A.; validation, W.M.L. and A.M.; formal analysis, W.M.L., A.C.M. and J.C.; investigation, W.M.L., A.C.M. and J.C.; resources, I.I.T.; data curation, W.M.L.; writing—original draft preparation, W.M.L.; writing—review and editing, A.C.M., A.H. and W.M.L.; visualization, W.M.L. and A.C.M.; supervision, A.H.; project administration, A.H.; funding acquisition, A.H. All authors have read and agreed to the published version of the manuscript.

Funding: This research was conducted as part of a Ph.D. project funded by AkerBP.

Data Availability Statement: Not applicable.

Acknowledgments: We would like to express our deepest gratitude to sponsors from AkerBP who kindly provided funding and data necessary for this research. We would also like to thank Kingba Princewill, Ahmed Jama Ahmed, Elliot Foley and Fraser Scott for their outstanding work on their respective MSc projects, which helped further this research, and other staff at the University of Aberdeen, most notably John Still for his support with microprobe analysis.

Conflicts of Interest: The authors declare no conflict of interest. The funders provided some of the samples and data necessary for this study. After manuscript review, they agree with and support this publication and indicate that data shared herein is not to be held in confidentiality.

References

1. Den Hartog Jager, D.; Giles, M.R.; Griffiths, G.R. Evolution of Paleogene submarine fans of the North Sea in space and time. *Geol. Soc. Lond. Pet. Geol. Conf. Ser.* **1993**, *4*, 59–71. [[CrossRef](#)]
2. Ahmadi, Z.M.; Sawyers, M.; Kenyon-Roberts, S.; Stanworth, C.W.; Kugler, K.A.; Kristensen, J.; Fugelli, E.M.G. Paleocene. In *The Millennium Atlas: Petroleum Geology of the Central and Northern North Sea*, 1st ed.; Evans, D., Graham, C., Armour, A., Bathurst, P., Eds.; The Geological Society of London: London, UK, 2003; pp. 215–259.
3. Brunstad, H.; Gradstein, F.; Vergara, L.; Lie, J.E.; Hammer, Ø. *A Revision of the Rogaland Group, Norwegian North Sea*; University of Oslo: Oslo, Norway, 2009.
4. Eldrett, J.; Tripsanas, E.; Davis, C.; McKie, T.; Vieira, M.; Osterloff, P.; Sandison, T. Sedimentological evolution of Sele Formation deep-marine depositional systems of the Central North Sea. *Geol. Soc. Lond. Spec. Publ.* **2015**, *403*, 63–98. [[CrossRef](#)]

5. Hurst, A.; Cartwright, J. (Eds.) *Sand Injectites: Implications for Hydrocarbon Exploration and Production*, AAPG Memoir 87; American Association of Petroleum Geologists: Tulsa, OK, USA, 2007.
6. Huuse, M.; Jackson, C.A.; Van Rensbergen, P.; Davies, R.J.; Flemings, P.B.; Dixon, R.J. Subsurface sediment remobilization and fluid flow in sedimentary basins: An overview. *Basin Res.* **2010**, *22*, 342–360. [[CrossRef](#)]
7. Duranti, D. Large-scale Sand Injection in the Paleogene of the North Sea: Modeling of Energy and Flow Velocities. In *Sand Injectites: Implications for Hydrocarbon Exploration and Production*; Cartwright, J.; Hurst, A., Eds.; American Association of Petroleum Geologists: Tulsa, OK, USA, 2007; Volume AAPG Memoir 87, pp. 129–139.
8. Huuse, M.; Cartwright, J.; Gras, R.; Hurst, A. Kilometre-scale sandstone intrusions in the Eocene of the Outer Moray Firth (UK North Sea): Migration paths, reservoirs and potential drilling hazards. *Pet. Geol. Conf. Proc.* **2005**, *6*, 1577–1594. [[CrossRef](#)]
9. Hurst, A.; Cartwright, J.; Duranti, D.; Huuse, M.; Nelson, M. Sand injectites: An emerging global play in deep-water clastic environments. *Pet. Geol. Conf. Proc.* **2005**, *6*, 133–144. [[CrossRef](#)]
10. Hurst, A.; Huuse, M.; Duranti, D.; Vigorito, M.; Jameson, E.; Schwab, A. Application of outcrop analogues in successful exploration of a sand injection complex, Volund Field, Norwegian North Sea. *Geol. Soc. Spec. Publ.* **2016**, *436*, 75–92. [[CrossRef](#)]
11. Szarawarska, E.; Huuse, M.; Hurst, A.; de Boer, W.; Lu, L.; Molyneux, S.; Rawlinson, P.B. Three-dimensional seismic characterisation of large-scale sandstone intrusions in the lower Palaeogene of the North Sea: Completely injected vs. in situ remobilised sandbodies. *Basin Res.* **2010**, *22*, 517–532. [[CrossRef](#)]
12. Schwab, A.; Jameson, E.; Townsley, A. Volund Field: Development of an Eocene sandstone injection complex, offshore Norway. *Geol. Soc. Spec. Publ.* **2015**, *403*, 247–260. [[CrossRef](#)]
13. White, N.; Lovell, B. Measuring the pulse of a plume with the sedimentary record. *Nature* **1997**, *387*, 888–891. [[CrossRef](#)]
14. Morton, A.C.; Hallsworth, C.; Wilkinson, G.C. Stratigraphic evolution of sand provenance during Paleocene deposition in the Northern North Sea area. *Geol. Soc. Lond. Pet. Geol. Conf. Ser.* **1993**, *4*, 73–84. [[CrossRef](#)]
15. Morton, A.C. Lower Tertiary Sand Development in Viking Graben, North Sea. *AAPG Bull.* **1982**, *66*, 1542–1559.
16. Hurst, A.; Morton, A.C. Provenance models: The role of sandstone mineral-chemical stratigraphy. *Geol. Soc. Spec. Publ.* **2014**, *386*, 7–26. [[CrossRef](#)]
17. Humphreys, B.; Morton, A.C.; Hallsworth, C.; Gatliff, R.W.; Riding, J.B. An integrated approach to provenance studies: A case example from the Upper Jurassic of the Central Graben, North Sea. *Geol. Soc. Spec. Publ.* **1991**, *57*, 251–262. [[CrossRef](#)]
18. Morton, A.C. The provenance and distribution of the Palaeocene sands of the central North Sea. *J. Pet. Geol.* **1979**, *2*, 11–21. [[CrossRef](#)]
19. Morton, A.C. Value of heavy minerals in sediments and sedimentary rocks for provenance, transport history and stratigraphic correlation. *Mineral. Assoc. Can. Short Course Ser.* **2012**, *42*, 133–165.
20. Morton, A.C.; McFadyen, S.; Hurst, A.; Pyle, J.; Rose, P. Constraining the origin of reservoirs formed by sandstone intrusions: Insights from heavy mineral studies of the Eocene in the Forties area, United Kingdom central North Sea. *AAPG Bull.* **2014**, *98*, 545–561. [[CrossRef](#)]
21. Hurst, A.; Morton, A.C.; Scott, A.; Vigorito, M.; Frei, D. Heavy-mineral assemblages in sandstone intrusions: Panoche giant injection complex, California, U.S.A. Panoche. *J. Sediment. Res.* **2017**, *87*, 388–405. [[CrossRef](#)]
22. Morton, A.C.; Hallsworth, C. Processes controlling the composition of heavy mineral assemblages in sandstones. *Sediment. Geol.* **1999**, *124*, 3–29. [[CrossRef](#)]
23. Garzanti, E.; Andò, S. Plate Tectonics and Heavy Mineral Suites of Modern Sands. *Dev. Sedimentol.* **2007**, *58*, 741–763. [[CrossRef](#)]
24. Garzanti, E.; Padoan, M.; Andò, S.; Resentini, A.; Vezzoli, G.; Lustrino, M. Weathering and Relative Durability of Detrital Minerals in Equatorial Climate: Sand Petrology and Geochemistry in the East African Rift. *J. Geol.* **2013**, *121*, 547–580. [[CrossRef](#)]
25. Morton, A.C. Stability of detrital heavy minerals in Tertiary sandstones from the North Sea basin. *Clay Miner.* **1984**, *19*, 287–308. [[CrossRef](#)]
26. Morton, A.C.; Hallsworth, C. Stability of Detrital Heavy Minerals During Burial Diagenesis. *Dev. Sedimentol.* **2007**, *58*, 215–245.
27. Morton, A.C. Influences of provenance and diagenesis on detrital garnet suites in the Paleocene Forties Sandstone, central North Sea. *J. Sediment. Res.* **1987**, *57*, 1027–1032.
28. Morton, A.C.; Hallsworth, C.; Chalton, B. Garnet compositions in Scottish and Norwegian basement terrains: A framework for interpretation of North Sea sandstone provenance. *Mar. Pet. Geol.* **2004**, *21*, 393–410. [[CrossRef](#)]
29. Morton, A.C. A new approach to provenance studies: Electron microprobe analysis of detrital garnets from Middle Jurassic sandstones of the northern North Sea. *Sedimentology* **1985**, *32*, 553–566. [[CrossRef](#)]
30. Kilhams, B.; Morton, A.C.; Borella, R.; Wilkins, A.; Hurst, A. Understanding the provenance and reservoir quality of the Sele Formation sandstones of the UK Central Graben utilizing detrital garnet suites. *Geol. Soc. Spec. Publ.* **2014**, *386*, 129–142. [[CrossRef](#)]
31. Morton, A.C.; Hallsworth, C. Identifying provenance-specific features of detrital heavy mineral assemblages in sandstones. *Sediment. Geol.* **1994**, *90*, 241–256. [[CrossRef](#)]
32. Mange, M.A.; Morton, A.C. Geochemistry of Heavy Minerals. *Dev. Sedimentol.* **2007**, *58*, 345–391.
33. Zanella, E.; Coward, M.P. Structural framework. In *The Millennium Atlas: Petroleum Geology of the Central and Northern North Sea*, 1st ed.; Evans, D., Graham, C., Armour, A., Bathurst, P., Eds.; The Geological Society of London: London, UK, 2003; Volume 45, pp. 45–59.
34. Badley, M.E.; Price, J.D.; Rambech Dahl, C.; Agdestein, T. The structural evolution of the northern Viking Graben and its bearing upon extensional modes of basin formation. *J. Geol. Soc.* **1988**, *145*, 455–472. [[CrossRef](#)]
35. Bryn, B.K.L.; Ackers, M.A. Unravelling the nature of deep-marine sandstones through the linkage of seismic geomorphologies to sedimentary facies; the Hermod Fan, Norwegian North Sea. In *From Depositional Systems to Sedimentary Successions on the*

- Norwegian Continental Margin*, 1st ed.; Martinius, A.W., Ravnås, R., Howell, J.A., Steel, R.J., Wonham, J.P., Eds.; International Association of Sedimentologists: Chichester, UK, 2014; Volume 9781118920466, pp. 647–676.
36. Hadler-Jacobsen, F.; Johannessen, E.P.; Ashton, N.; Henriksen, S.; Johnson, S.D.; Kristensen, J.B. Submarine fan morphology and lithology distribution: A predictable function of sediment delivery, gross shelf-to-basin relief, slope gradient and basin topography. *Pet. Geol. Conf. Proc.* **2005**, *6*, 1121–1145. [[CrossRef](#)]
 37. Jones, E.; Jones, R.; Ebdon, C.; Ewen, D.; Milner, P.; Plunkett, J.; Hudson, G.; Slater, P. Eocene. In *The Millennium Atlas: Petroleum Geology of the Central and Northern North Sea*, 1st ed.; Evans, D., Graham, C., Armour, A., Bathurst, P., Eds.; The Geological Society of London: London, UK, 2003; pp. 261–277.
 38. McKie, T.; Rose, P.T.S.; Hartley, A.J.; Jones, D.W.; Armstrong, T.L. Tertiary deep-marine reservoirs of the North Sea region: An introduction. *Geol. Soc. Spec. Publ.* **2015**, *403*, 1–16. [[CrossRef](#)]
 39. Mudge, D.C.; Copestake, P. Lower Palaeogene stratigraphy of the northern North Sea. *Mar. Pet. Geol.* **1992**, *9*, 287–301. [[CrossRef](#)]
 40. Deegan, C.E.; Scull, B.J. *A Standard Lithostratigraphic Nomenclature for the Central and Northern North Sea*; Norwegian Petroleum Directorate Bulletin: Stavanger, Norway, 1977; Volume 1.
 41. Dixon, R.J.; Pearce, J. Tertiary sequence stratigraphy and play fairway definition, Bruce-Beryl Embayment, Quadrant 9, UKCS. *Nor. Pet. Soc. Spec. Publ.* **1995**, *5*, 443–469. [[CrossRef](#)]
 42. Ichron Ltd. *Stratigraphic Correlation of Boyla-Caterpillar Wells*; Ichron Ltd: Rudheath, UK, 2011.
 43. Biostrat: Wells and Samples. Available online: http://nhm2.uio.no/norges/full/sample_data.php? (accessed on 5 July 2021).
 44. Skjærpe, I.; Tøllefsen, I.; Endresen, T. *Developing Viper-Kobra: Maximizing Recovery by Exploiting the Unique Characteristics of the Sand Injectite Environment*; European Association of Geoscientists & Engineers: Bunnik, The Netherlands, 2018.
 45. Flinn, D. *Interpretative Map of Shetland Geology*; Hall Publishing: Hoboken, NJ, USA, 2014.
 46. Read, H.H. The Metamorphic Geology of Unst in the Shetland Islands. *Q. J. Geol. Soc.* **1934**, *90*, 637–688. [[CrossRef](#)]
 47. Read, H.H. The metamorphic history of Unst, Shetland. *Proc. Geol. Assoc.* **1936**, *47*, 283–293. [[CrossRef](#)]
 48. Flinn, D.; Miller, J.A.; Roddom, D. The age of the Norwick hornblende schists of Unst and Fetlar and the obduction of the Shetland ophiolite. *Scott. J. Geol.* **1991**, *27*, 11–19. [[CrossRef](#)]
 49. Spray, J.G. Thrust-related metamorphism beneath the Shetland Islands oceanic fragment, northeast Scotland. *Can. J. Earth Sci.* **1988**, *25*, 1760–1776. [[CrossRef](#)]
 50. Chesher, J.A. *Geology of the United Kingdom, Ireland and the Adjacent Continental Shelf (North Sheet)*; British Geological Survey: Nottingham, UK, 1991.
 51. Mange, M.A.; Maurer, H. *Heavy Minerals in Colour*; Springer: Dordrecht, The Netherlands, 2012.
 52. Galehouse, J.S. Point Counting. In *Procedures in Sedimentary Petrology*, 1st ed.; Carver, R.E., Ed.; Wiley Interscience: London, UK, 1971; pp. 385–408.
 53. Morton, A.C.; Hallsworth, C.; Kunka, J.; Ewan, L.; Payne, S.; Walder, D. Heavy-mineral stratigraphy of the Clair Group (Devonian–Carboniferous) in the Clair Field, West of Shetland, U.K. In *Application of Modern Stratigraphic Techniques: Theory and Case Histories*; Ratcliffe, K.T., Zaitlin, B.A., Eds.; Society for Sedimentary Geology: Tulsa, OK, USA, 2010; Volume 94, pp. 183–199.
 54. Krippner, A.; Meinhold, G.; Morton, A.C.; Von Eynatten, H. Evaluation of garnet discrimination diagrams using geochemical data of garnets derived from various host rocks. *Sediment. Geol.* **2014**, *306*, 36–52. [[CrossRef](#)]
 55. Jolley, D.W.; Morton, A.C. Understanding basin sedimentary provenance: Evidence from allied phytogeographic and heavy mineral analysis of the Palaeocene of the NE Atlantic. *J. Geol. Soc.* **2007**, *164*, 553–563. [[CrossRef](#)]
 56. Ichron Ltd. *Sedimentology, Petrography and Reservoir Quality of the Cored Hermod (Palaeocene) Interval in Well 24/9-10S, Norwegian North Sea*; Ichron Ltd: Rudheath, UK, 2012.
 57. Enjolras, J.M.; Gouadain, J.; Mutti, E.; Pizon, J. New turbiditic model for the Lower Tertiary sands in the South Viking Graben. In *Proceedings of the Habitat of Hydrocarbons on the Norwegian Continental Shelf*, International Conference, 1–3 October 1985; Spencer, A.M., Ed.; Graham & Trotman: Totnes, UK, 1986; pp. 171–178.
 58. Mudge, D.C. Regional controls on Lower Tertiary sandstone distribution in the North Sea and NE Atlantic margin basins. *Geol. Soc. Spec. Publ.* **2015**, *403*, 17–42. [[CrossRef](#)]
 59. McInerney, F.A.; Wing, S.L. The Paleocene-Eocene Thermal Maximum: A Perturbation of Carbon Cycle, Climate, and Biosphere with Implications for the Future. *Annu. Rev. Earth Planet. Sci.* **2011**, *39*, 489–516. [[CrossRef](#)]
 60. Foreman, B.Z.; Heller, P.L.; Clementz, M.T. Fluvial response to abrupt global warming at the Palaeocene/Eocene boundary. *Nature* **2012**, *491*, 92–95. [[CrossRef](#)] [[PubMed](#)]
 61. Kemp, S.J.; Ellis, M.A.; Mountney, I.; Kender, S. Palaeoclimatic implications of high-resolution clay mineral assemblages preceding and across the onset of the Palaeocene-Eocene Thermal Maximum, North Sea Basin. *Clay Min.* **2016**, *51*, 793–813. [[CrossRef](#)]
 62. Gibson, T.G.; Bybell, L.M.; Mason, D.B. Stratigraphic and climatic implications of clay mineral changes around the Paleocene/Eocene boundary of the northeastern US margin. *Sediment. Geol.* **2000**, *134*, 65–92. [[CrossRef](#)]
 63. Robert, C.; Kennett, J.P. Antarctic subtropical humid episode at the Paleocene-Eocene boundary: Clay-mineral evidence. *Geology* **1994**, *22*, 211–214. [[CrossRef](#)]
 64. Bowen, G.J.; Beerling, D.J.; Koch, P.L.; Zachos, J.C.; Quattlebaum, T. A humid climate state during the Palaeocene/Eocene thermal maximum. *Nature* **2004**, *432*, 495–499. [[CrossRef](#)]
 65. Pujalte, V.; Schmitz, B.; Baceta, J.I. Sea-level changes across the Paleocene–Eocene interval in the Spanish Pyrenees, and their possible relationship with North Atlantic magmatism. *Palaeogeogr. Palaeoclimatol. Palaeoecol.* **2014**, *393*, 45–60. [[CrossRef](#)]

66. Nagy, J.; Jargvoll, D.; Dypvik, H.; Jochmann, M.; Riber, L. Environmental changes during the Paleocene–Eocene Thermal Maximum in Spitsbergen as reflected by benthic foraminifera. *Polar Res.* **2013**, *32*, 19737. [[CrossRef](#)]
67. Kender, S.; Stephenson, M.H.; Riding, J.B.; Leng, M.J.; Knox, R.W.O.; Peck, V.L.; Kendrick, C.P.; Ellis, M.A.; Vane, C.H.; Jamieson, R. Marine and terrestrial environmental changes in NW Europe preceding carbon release at the Paleocene–Eocene transition. *Earth Planet. Sci. Lett.* **2012**, *353*, 108–120. [[CrossRef](#)]
68. Hubert, J.F. A Zircon-Tourmaline-Rutile Maturity Index and the Interdependence of the Composition of Heavy Mineral Assemblages with the Gross Composition and Texture of Sandstones. *J. Sediment. Res.* **1962**, *32*, 440–450.
69. Hallsworth, C.R.; Morton, A.C.; Dore, G. Contrasting mineralogy of Upper Jurassic sandstones in the Outer Moray Firth, North Sea: Implications for the evolution of sediment dispersal patterns. *Geol. Soc. Lond. Spec. Publ.* **1996**, *114*, 131–144. [[CrossRef](#)]
70. Morton, A.C.; Herries, R.; Fanning, M. Correlation of Triassic Sandstones in the Strathmore Field, West of Shetland, Using Heavy Mineral Provenance Signatures. *Dev. Sedimentol.* **2007**, *58*, 1037–1072. [[CrossRef](#)]
71. Andrews, S.D.; Morton, A.C.; Decou, A.; Frei, D. Reconstructing drainage pathways in the North Atlantic during the Triassic utilizing heavy minerals, mineral chemistry, and detrital zircon geochronology. *Geosphere* **2021**, *17*, 479–500. [[CrossRef](#)]